

Copyright Warning & Restrictions

The copyright law of the United States (Title 17, United States Code) governs the making of photocopies or other reproductions of copyrighted material.

Under certain conditions specified in the law, libraries and archives are authorized to furnish a photocopy or other reproduction. One of these specified conditions is that the photocopy or reproduction is not to be “used for any purpose other than private study, scholarship, or research.” If a user makes a request for, or later uses, a photocopy or reproduction for purposes in excess of “fair use” that user may be liable for copyright infringement,

This institution reserves the right to refuse to accept a copying order if, in its judgment, fulfillment of the order would involve violation of copyright law.

Please Note: The author retains the copyright while the New Jersey Institute of Technology reserves the right to distribute this thesis or dissertation

Printing note: If you do not wish to print this page, then select “Pages from: first page # to: last page #” on the print dialog screen

The Van Houten library has removed some of the personal information and all signatures from the approval page and biographical sketches of theses and dissertations in order to protect the identity of NJIT graduates and faculty.

INFORMATION TO USERS

This was produced from a copy of a document sent to us for microfilming. While the most advanced technological means to photograph and reproduce this document have been used, the quality is heavily dependent upon the quality of the material submitted.

The following explanation of techniques is provided to help you understand markings or notations which may appear on this reproduction.

1. The sign or "target" for pages apparently lacking from the document photographed is "Missing Page(s)". If it was possible to obtain the missing page(s) or section, they are spliced into the film along with adjacent pages. This may have necessitated cutting through an image and duplicating adjacent pages to assure you of complete continuity.
2. When an image on the film is obliterated with a round black mark it is an indication that the film inspector noticed either blurred copy because of movement during exposure, or duplicate copy. Unless we meant to delete copyrighted materials that should not have been filmed, you will find a good image of the page in the adjacent frame. If copyrighted materials were deleted you will find a target note listing the pages in the adjacent frame.
3. When a map, drawing or chart, etc., is part of the material being photographed the photographer has followed a definite method in "sectioning" the material. It is customary to begin filming at the upper left hand corner of a large sheet and to continue from left to right in equal sections with small overlaps. If necessary, sectioning is continued again—beginning below the first row and continuing on until complete.
4. For any illustrations that cannot be reproduced satisfactorily by xerography, photographic prints can be purchased at additional cost and tipped into your xerographic copy. Requests can be made to our Dissertations Customer Services Department.
5. Some pages in any document may have indistinct print. In all cases we have filmed the best available copy.

University
Microfilms
International

300 N. ZEEB RD., ANN ARBOR, MI 48106

8121967

GELBER, MELVIN WILBUR

DEPOSITION OF PARTICLES IN VERTICAL CONDUITS DUE TO
ELECTROSTATIC CHARGE, DIFFUSION, AND GRAVITY

New Jersey Institute of Technology

D.ENG.SC.

1981

University
Microfilms
International

300 N. Zeeb Road, Ann Arbor, MI 48106

PLEASE NOTE:

In all cases this material has been filmed in the best possible way from the available copy. Problems encountered with this document have been identified here with a check mark .

1. Glossy photographs or pages _____
2. Colored illustrations, paper or print _____
3. Photographs with dark background _____
4. Illustrations are poor copy _____
5. Pages with black marks, not original copy _____
6. Print shows through as there is text on both sides of page _____
7. Indistinct, broken or small print on several pages
8. Print exceeds margin requirements _____
9. Tightly bound copy with print lost in spine _____
10. Computer printout pages with indistinct print _____
11. Page(s) _____ lacking when material received, and not available from school or author.
12. Page(s) _____ seem to be missing in numbering only as text follows.
13. Two pages numbered _____. Text follows.
14. Curling and wrinkled pages _____
15. Other _____

University
Microfilms
International

DEPOSITION OF PARTICLES IN VERTICAL CONDUITS
DUE TO
ELECTROSTATIC CHARGE, DIFFUSION, AND GRAVITY

BY
MELVIN WILBUR GELBER

A DISSERTATION
PRESENTED IN PARTIAL FULFILLMENT OF THE
REQUIREMENTS FOR THE DEGREE OF
DOCTOR OF ENGINEERING SCIENCE IN
MECHANICAL ENGINEERING

AT
NEW JERSEY INSTITUTE OF TECHNOLOGY

This dissertation is to be used only with due regard to the rights of the author. Bibliographical references may be noted, but passages must not be copied without permission of the Institute and without credit being given in subsequent written or published word.

Newark, New Jersey
1981

ABSTRACT

This investigation was made to determine the effect on the deposition of fine particles in a vertical channel and in a vertical tube due to the influences of electrostatic charge, diffusion, and gravity acting in the direction of flow. The flow considered was laminar, incompressible and steady.

The governing equations for the fluid phase were derived from the Navier-Stokes equation and the continuity equation while the equations for the particle phase were derived from Poisson's potential equation and the continuity equation. Since the governing equations are non-linear partial differential equations the solutions were developed using numerical methods.

The flow patterns considered were uniform, developing and fully developed with symmetry about the axis of the channel or tube.

For the case of channel flow, variations in deposition were determined using an axial parameter which included a ratio of the electrostatic charge to the diffusion effect. The results were obtained along the channel for various values of electrostatic charge. The deposition due to diffusion and charge effect was studied and the range of charge effect was determined for which the diffusion effect may be neglected. Also, the deposition due to charge and gravity was investigated to determine the effect of the velocity profile on the deposition. It was found that when the velocity ratio is greater than 10 the deposition

was not greatly affected by the velocity profile.

For the case of the vertical tube, it was found that the deposition depends on the velocity ratio of terminal velocity to the average fluid velocity and decreases with increasing velocity ratio. The curves for the fraction of deposition at any velocity ratio were found to fall between that for uniform flow and that for fully developed flow due to diffusive effect alone when a proper dimensionless distance was used.

APPROVAL OF DISSERTATION

DEPOSITION OF PARTICLES IN VERTICAL CONDUITS

DUE TO

ELECTROSTATIC CHARGE, DIFFUSION, AND GRAVITY

BY

MELVIN WILBUR GELBER

FOR

DEPARTMENT OF MECHANICAL ENGINEERING

NEW JERSEY INSTITUTE OF TECHNOLOGY

BY

FACULTY COMMITTEE

APPROVED: _____ CHAIRMAN

NEWARK, NEW JERSEY
1981

ACKNOWLEDGEMENTS

The author wishes to acknowledge his indebtedness to Professor Rong-Yaw Chen, advisor and project director. Professor Chen is deserving of the most sincere gratitude for his kindness, patience and guidance through the pursuit of this study. It is rewarding to the author to have experienced this association.

The author also wishes to express his gratitude to Professors John V. Droughton, Hans E. Pawel, Roman I. Andrushkiw and Henry S. Kao, who have kindly given their time and assistance in reading the original manuscript and in providing many constructive and valuable suggestions.

My sincere gratitude also to Mrs. Arthur Bayen for her patience and her assistance in the typing of this manuscript.

TABLE OF CONTENTS

	Page
ABSTRACT	i
APPROVAL PAGE	iii
ACKNOWLEDGEMENTS	iv
TABLE OF CONTENTS	v
LIST OF FIGURES	vii
NOMENCLATURE	ix
1. INTRODUCTION	1
2. LITERATURE SURVEY ON THE DEPOSITION OF PARTICLES	4
3. LAMINAR FLOW OF PARTICLES IN A PARALLEL-PLATE CHANNEL WITH ELECTROSTATIC CHARGE, DIFFUSION, AND GRAVITATIONAL EFFECTS	15
3.1 General Description	15
3.2 Governing Equations	16
3.3 Analysis for Diffusion and Electrostatic Charge	20
3.4 Analysis for Electrostatic Charge Only	22
3.5 Analysis for Electrostatic Charge With Gravity in the Direction of Flow	25
3.6 Results and Discussion	27
4. THE EFFECT OF THE TERMINAL VELOCITY AND THE EFFECT OF THE VELOCITY DEVELOPMENT ON THE DEPOSITION IN A VERTICAL CIRCULAR TUBE	31
4.1 General Description	31

4.2	Governing Equations	32
4.3	Analysis of Solution	34
4.4	Results and Discussion	37
5.	CONCLUSIONS	39
6.	RECOMMENDATIONS	43
	REFERENCES	44
	Appendix	
A.	DIMENSIONLESS QUANTITIES AND PARAMETERS	46
B.	NON-DIMENSIONALIZATION AND SIMPLIFICATION OF GOVERNING EQUATIONS	49
C.	NUMERICAL PROCEDURE FOR SOLVING THE EQUATIONS IN CHAPTERS 3 AND 4	56
	FIGURE	74
	VITA	88

LIST OF FIGURES

Figure		Page
3.1	Vertical Parallel Plate Channel Configuration.....	74
3.2	Computer Flow Chart for Flow in a Parallel Plate Channel for Diffusion and Electrostatic Charge.....	75
3.3	Axial Distribution of Fraction of Penetration due to Diffusion and Charge Effect for Uniform Flow in a Channel with X as Axial Parameter.....	76
3.4	Axial Distribution of Fraction of Penetration due to Diffusion and Charge Effect for Uniform Flow in a Channel with $4\alpha X/\beta$ as Axial Parameter	77
3.5	Axial Distribution of Fraction of Penetration due to Diffusion and Charge Effect for Parabolic Flow in a Channel with X as Axial Parameter	78
3.6	Axial Distribution of Fraction of Penetration due to Diffusion and Charge Effect for Parabolic Flow in a Channel with $4\alpha X/\beta$ as Axial Parameter	79
3.7	Axial Distribution of Fraction of Penetration due to Charge and Gravity Effects in a Vertical Channel	80
3.8	Test Data - Fraction of Deposition for Vertical Tube due to Charge and Gravity Effect for Uniform Flow	81
4.1	Finite Difference Representation of Flow Field Showing Axial and Radial Increments	82
4.2	Computer Flow Chart for Flow in a Vertical Circular Tube with Diffusion and Gravity Effects	83

4.3	Axial Distribution of Fraction of Deposition with Varying Gravity Flow Parameters of $\xi = 0, 1, 10$ and Varying Schmidt Numbers of $Sc = 0.0, 0.1, 1.0,$ and ∞ for Flow in a Circular Tube	84
4.4	Axial Distribution of Fraction of Penetration with Varying Velocity Ratio Parameter for Fully Developed Flow and with Uniform Flow in a Circular Tube	35
4.5	Axial Distribution of Fraction of Deposition with Varying Gravity Flow Parameters of $\xi = 0, 1, 10$ and Varying Schmidt Numbers of $Sc = 0.0, 0.1, 1.0,$ and ∞ for Flow in a Parallel Plate Channel	86
4.6	Axial Distribution of Fraction of Penetration with Varying Velocity Ratio Parameter for Fully Developed Flow and with Uniform Flow in a Parallel Plate Channel	87

NOMENCLATURE

e_x	axial component of electric field intensity
e_y	normal component of electric field intensity
h	half width of channel
m_p	particle mass
p	fluid static pressure
q	electric charge on particle
r	radial distance from axis of tube
r_0	radius of tube
u	axial component of fluid velocity
u_0	uniform inlet velocity of fluid
u_p	axial component of particle velocity
v_p	normal component of particle velocity
v_g	terminal particle velocity in the axial direction
x, y	axial and normal coordinates
D	particle diffusivity
E	dimensionless electric field intensity
E^*	dimensionless electric field intensity
F	inverse of relaxation time for momentum transfer
J_{px}	mass flux in x - direction
J_{py}	mass flux in y - direction
R	dimensionless particle concentration
U	dimensionless axial component of fluid velocity
V	dimensionless normal component of fluid velocity
X, Y	dimensionless axial and normal coordinates

X^*_1	dimensionless axial coordinate
X^*_2	dimensionless axial coordinate

Superscripts and Subscripts

*	dimensionless quantity
c	centerline condition
i, j	coordinates on finite difference grid
o	inlet condition
p	particle phase

Greek Letters

α	electrostatic charge parameter
β	diffusive peclet number
S	velocity ratio
ϵ_0	free space permittivity
ρ_p	particle concentration
ρ_{p0}	inlet particle concentration
μ	viscosity of fluid
ρ	density of fluid phase
$\bar{\rho}_p$	particle density

1. INTRODUCTION

The deposition of particles in suspension of moving fluids deals with the mechanics of two phase fluid - solid systems. The investigation of such systems is of practical importance as it has so many common applications. These may be experienced in such industrial applications as aerosol sprays, boiler exhaust gas, dust collection equipment, pollution control exhaust and particle emission of internal combustion engine exhaust systems. Other applicable examples are deposition of aerosols in the human respiratory tract and the flow of blood in the circulatory system. It is the deposition of the particles with which we are concerned. In some cases such as with dust collectors the process is desirable while in others such as the respiratory tract the process is detrimental. The significance of analytical study such as this is to develop a mathematical model so as to make a reliable prediction of the performance involved.

The main object of this study is to investigate the effect on the deposition of particles in a vertical tube and a vertical channel due to the influences of electrostatic charge, diffusion and gravity. The study was made for laminar, incompressible steady flow. Since the governing equations are non-linear partial differential equations, numerical methods were used to develop the solution. Due to the selection of vertical tubes and channels the patterns will be considered symmetrical about the axis. The velocity profiles were assumed to be uniform for plug flow and parabolic for fully developed flow. The electrostatic

charge is considered to be generated by collision between the solid particles themselves and between the solid particles and the channel or tube wall.

In one case the vertical tube is considered with developing flow in the entrance of the tube. A particular object of this study is to determine the effect of the velocity development when diffusion and gravity are considered with no electrostatic charge.

Another particular object of this study is to determine the deposition due to electrostatic charge and diffusion effects and compare this with that due to electrostatic charge alone. The purpose is to determine the range of charge effect for which the diffusive effect may be neglected. Since the diffusive term is the only second order term in the governing partial differential equation the conditions under which it may be eliminated will determine when the governing equation can be reduced to a first order equation and allow a more simple solution.

A third particular objective is to determine the effect of the terminal velocity of the particles on the deposition in a vertical channel or circular tube. It is intended to find the required conditions which if the diffusive effect is neglected and only the electrostatic charge and gravity effects are considered, that the deposition is not greatly affected by the velocity profile. Under such conditions the velocity profile may be simply assumed to be that for uniform flow.

In Chapter 2 a brief literature survey on the deposition of

suspensions on the internal surfaces of tubes and channels was studied. In Chapter 3 the laminar flow of particles in a parallel plate channel with electrostatic charge, diffusion and gravitational effects was studied including the effects of the several combinations of these forces. In Chapter 4 the effect of the terminal velocity and also the effect of the velocity profile on the deposition in a vertical tube was studied. Conclusions are presented in Chapter 5 and suggested recommendations for future study are presented in Chapter 6.

2. LITERATURE SURVEY

The flow of suspensions of particles and their deposition has been studied by many investigators. This survey briefly reviews the literature reported on the problem of flow within tubes and channels for laminar flows of aerosols which are influenced by the effects of diffusion, electrostatic force and gravity.

Taulbee [1] studied the deposition of particles due to simultaneous settling and diffusion from slug or Poiseuille flow in a horizontal parallel plate channel. He presented solutions for deposition and bulk mean concentration variations along the channel for the case when settling is large compared to the diffusion. The bulk mean concentration is the ratio of concentration at any distance from the axis to the concentration at the channel entrance.

In this paper Taulbee referred to Ingham's papers [10, 11] which presented a Fourier series solution for slug flow, a numerical solution for small σ ($v_g h/D$ gravity flow parameter), and asymptotic series solutions which are valid for small axial distance and which converge only for small σ . Taulbee shows that Ingham's solutions for large σ are incorrect. Discussing solutions presented by Taulbee and Yu [13] for slug flow, Ingham shows these to be correct.

For a horizontal parallel plate channel Taulbee's equation is

$$u \frac{\partial c}{\partial x} = D \frac{\partial^2 c}{\partial y^2} + v_g \frac{\partial c}{\partial y^2}$$

Using Laplace transforms he obtains exact solutions near the top wall and near the bottom wall. These solutions

are valid for all values of the gravity flow parameter σ at any axial distance as long as there is a core of uniform concentration between the top and bottom boundary layers. He compared his solution with the Fourier series solution given by Taulbee and Yu [13] and the results were practically identical. Taulbee also presented a series solution for Poiseuille flow using similar procedures as did Ingham [11].

Next, eliminating a term in his assumed velocity profile, since significant concentration variations take place near the walls where the profile is linear, he solved the equation using numerical methods which also give almost identical results with the series solution.

These results are valid for any axial distance and for any combination of diffusion and settling for a horizontal channel for both slug and Poiseuille flow.

Ingham [2] studied the diffusion of aerosols in a long cylindrical channel. He considered that for particles flowing through the channel the Brownian motion, or diffusion, of the particles may bring them in contact with the tube wall where they are absorbed or lose their charge. In his governing equation he included a term q representing the rate of formation of aerosols per unit volume but in his solution assumed q to be zero. He further assumed that the diffusive mass transfer along the tube in the direction of the flow may be neglected and radial velocity to be zero. He solved the equation analytically in terms of one parameter ∇ , where $\nabla \equiv DL/4U\lambda_0^2$. D = coefficient of diffusion of the particles, L = tube length, U = mean axial velocity of fluid, λ_0 = tube radius. The equation was solved using a series solution for

Poiseuille flow, plug flow, and a combination of both such that an allowance for slip velocity at the wall may be taken into account.

For small values of ∇ (0 to 0.1) Ingham compared his results for the ratio of mean concentration leaving the tube to the mean concentration entering the tube with Davies [14] and Gormley & Kennedy [15].

For the case of Poiseuille flow he again solved the equation and compared his results with Davies, Gormley & Kennedy and Thomas [16].

Finally, assuming a velocity distribution including a slip factor developed by Smutek [17], he solved the equation and compared his results with Tau and Hsu [12].

Hornbeck [3] analyzed numerically the laminar flow of an incompressible fluid in the inlet of a pipe. Without linearizing assumptions or using different solutions in various regions of the flow field Hornbeck transformed the basic differential equation into a dimensionless form. Imposing a grid on the flow field he presented the equations in a finite difference form. Working with a basis mesh size of $\nabla R = 0.1$ in the radial direction, and $\nabla Z = 0.01$ in the axial direction he progressed downstream solving the equations. He found it necessary to use very small mesh sizes in regions of rapid velocity changes near the pipe wall. ($\nabla R = .025$ and $\nabla Z = 2.5 \times 10^{-5}$). He compared his results favorably with the analytical solutions of Campbell & Lattery [18] and Longhaar [19].

Ingham [4] considered the problem of the steady flow of suspensions

of electrostatically charged particles with diffusion near the entrance of a cylindrical tube. Neglecting axial diffusion, and with zero radial velocity his governing equations included the steady state transport equation and Poisson's equation for the electrostatic field. Ingham solved these equations analytically near the entrance. The purpose of his paper was to obtain an analytic solution which was valid near the entrance to the tube to the same problem as described by Chen [9] wherein Chen used the integral method, for both plug and Poiseuille flows.

Ingham first non-dimensionalized all quantities. For plug flow with the axial velocity $U = 1$, he assumed solutions near the entrance but away from the boundary layer which were independent of the radial distance from the axis. He then established a boundary layer to satisfy the condition where the non-dimensionalized particle concentration was zero. Substituting these assumed solutions into the governing equations he balanced the diffusion with the inertia term looking for a similarity solution. He next substituted these solutions into the governing equations and then assumed solutions in the form of a polynomial expansion. Finally, substituting these assumed solutions into the equation he collected the same order terms. Matching the boundary layer solution with the internal flow he arrived at new boundary conditions. The solution of these equations with the new boundary conditions led to a non-linear ordinary differential equation which he integrated numerically.

For Poiseuille flow, using a velocity profile of the form $U = (1 - \frac{r^2}{r_0^2})$ where r_0 is the tube radius, Ingham again assumed a series solution. The form, however, was different from that assumed by

Chen [9] in that Chen assumed that the particle density was independent of the radial position outside the boundary layer while Ingham assumed that it depended upon the radial distance. The results which Ingham obtained for zero electrostatic effect ($\alpha = 0$) compared favorably with results published by Gormley and Kennedy [15] and Ingham [2]. Increasing α results in increasing the deposition. As the value of α increases he found that the values of the non-dimensionalized tube length (X) for which the terminated series are valid decreases. For the smaller values of α he found that his analytic solution was in good agreement with Chen's [9] numerical solution for both plug and Poiseuille flow.

Chen [5] studied the diffusive deposition of particles in the entrance region of a channel using an integral method. Previous authors such as Fuchs [20] and Davies [14] had made studies on deposition of particles due to diffusion in a long channel and Taulbee and Yu [13] and Ingham [7] had studied simultaneous diffusion and sedimentation in a long channel. Their solutions were based on fully developed flow. In this paper Chen presented the effect of developing flow in the entrance region of a channel on the diffusive deposition of particles.

Working with the diffusion equation and the continuity equation the author proceeded to integrate the governing equations from the centerline of the channel to the wall. To complete the integration it was necessary to know the velocity distribution across the channel in the entrance region under consideration. This in turn required the solution of the continuity equation and the momentum equation for the fluid phase. This had previously been solved by Gupta [24] by an integral method

which imposes the condition that the pressure gradient in the x - direction calculated from the momentum considerations is equal to that calculated from mechanical energy considerations.

Thus, the velocity profile was assumed to be equal to 1 for $0 \ll Y \ll 1-M$ and equal to $1 - \left(\frac{Y-1+M}{M}\right)^2$ for $1-M \ll Y \ll 1$, where M is equal to the ratio of the hydrodynamic boundary layer to the half width of the channel.

A concentration profile was assumed in the form of a polynomial satisfying the boundary conditions. Then, the integral was reduced to an equation involving the diffusive deposition in the entrance region of the channel as a function of the Schmidt number (Peclet Number/ Reynolds Number = \mathcal{V}/D). Chen solved the differential equations using numerical methods.

The results of this investigation for Uniform flow were compared with the series solution of Carslaw and Jaeger [23] and the differences were small. The results of this work for fully developed flow compared closely with Kennedy [15] for small values of X (< 0.1) and favorably with De Marcus [25] for large values of X (> 0.1). In presenting the results for developing flow it was found that at low Schmidt numbers ($\ll 0.01$) the growth of the hydrodynamic boundary layer is so slow that the deposition approaches that of uniform flow; as X increases the boundary layer grows faster and deviates from that of uniform flow. At high Schmidt numbers (≥ 100) the deposition approaches that of fully developed flow since the flow becomes fully developed in a small distance X.

Chen and Korjak [6] investigated numerically the deposition of aerosols with gravity in a vertical channel from the inlet to a distance of 50 channel widths for developing, fully developed, and uniform laminar flows. The purpose of this study was to determine the relative importance of sedimentation as compared to Brownian diffusion using a parameter $\sigma = v_g h/D$ where v_g is the settling velocity, h is the half channel width, and D is the particle diffusivity.

The concentration distribution was found for various values of the gravity flow parameter σ and various values of the Schmidt Number (Pe/Re).

For a given gravity flow parameter σ , increasing the Schmidt Number increases the penetration or, increasing the ratio of viscous force to diffusive force increases the penetration (decreasing the deposition). Also, for a given gravity flow parameter, for the case of fully developed flow ($Sc = \infty$) the penetration is less than for the case of uniform flow ($Sc = 0$).

As the gravity flow parameter σ increases for any given Schmidt Number the penetration increases. Finally, as σ approaches ∞ , the penetration approaches 1. The case of $\sigma = 0$ (no gravity flow and the particle motion is due solely to diffusion), the results agreed with those found by Ingham [7] for fully developed and uniform flow.

Ingham [11] reported on simultaneous diffusion and sedimentation of aerosol particles in a rectangular tube where the tube is very wide

compared with the distance between the other walls and the short dimension of the channel parallel to gravity was investigated.

Previous authors had developed results of the effects of diffusive and sedimentation of aerosol particles from Poiseuille flow and plug flow in tubes and some of these results were compared with those of this author, Ingham.

Ingham placed emphasis on the case when the diffusive effects are larger than, or of the same order as sedimentation effects and developed single expressions for the concentration distributions at small distances down the tube and also for the mean concentrations.

For Poiseuille flow the author first non-dimensionalized the governing partial differential equation. Using the boundary conditions he assumed a similarity series solution. Collecting terms of the same order he arrived at a set of ordinary differential equations which he solved numerically. The result was an equation for the mean concentration of aerosol particles consisting of five terms where the variables were $s = \left(\frac{2D}{3Qh}\right)Z$, depending upon the coefficient of diffusion, D ; the rate of gas flowing through the tube per unit width, Q ; the half width of the tube, h ; and the axial distance, and the diffusion and sedimentation parameter $\alpha = \frac{hvg}{D}$. His equation compared closely with that of Gormley and Kennedy [15].

For plug flow, the author solved the governing equation with boundary conditions and arrived at an infinite series. This series solution was valid for all σ but if $\sigma \ll 0(1)$ a boundary layer analysis

can be made (original assumption that sedimentation does not dominate over diffusion) to obtain a solution near the entrance to the tube ($u = \text{non-dimensional distance along the tube} = \left(\frac{2D}{Qh}\right) Z$ such that the series solutions may be reduced to a solution of four terms). Thus, the mean concentration of aerosol particles was dependent on the diffusion and sedimentation parameter $\frac{(hv_g)}{2D}$ and u , the non-dimensional distance along the tube.

For both Poiseuille flow and plug flow Ingham tabulated his results and arrived at the following conclusions.

1. In both Poiseuille flow and plug flow the simplified expressions for the particle concentration were valid for small distances down the tube and gave accurate results with few terms required.
2. For Poiseuille flow it was impractical to take more than two terms for an equation he previously developed [10] and his simplified equation was more useful.
3. These simplified solutions were only valid for the case where diffusion dominates over sedimentation.
4. The numerical technique used was valid only for small values of the diffusion and sedimentation parameter σ since there were not sufficient mesh points in the very thin diffusion layers.
5. Finally, the equations were valid for the diffusion and sedimentation parameter $\sigma \ll 0(1)$.

Chen [8] studied the deposition of aerosols in a long channel due to diffusive and electrostatic charge effects by an integral method. The fluid phase was assumed to be either uniform flow or fully developed flow. Two methods were presented.

In the first method the author integrated the governing equations. Using a third order polynomial for the particle density and with the use of the boundary conditions he assumed the particle density profile near the inlet plane to be made of a uniform center core and a polynomial boundary layer. Introducing a new variable to denote the ratio of the thickness of the particle density boundary layer to the half channel width, a particle density profile was developed containing this variable and a coefficient to be determined from the diffusion equation through integration and the centerline condition. The equations were solved numerically and compared with a second method.

In the second method the author used a fully developed particle density profile. The equations were again solved numerically.

The results showed that the analysis for the second method gave the best results for uniform flow as compared with the series solution by Carslaw and Jaeger [23] , the author's first method, and a fourth order polynomial previously presented by Chen [5] . Comparison of results on fully developed flow also show that the second method was better than the first.

While the two methods showed considerable difference in deposition at $\alpha = 0$, this difference decreases as α increases until at $\alpha = 10$ the

difference is less than 0.008.

Finally, the results show that the centerline particle density, the penetration, and the electric field force decreased exponentially with the axial distance for flow far from the channel inlet.

Chen [9] studied the effects of diffusion and electrostatic charge in a circular tube and solved the equations with an integral method. Results were obtained for plug flow and Poiseuille flow. The transport equation and Poisson's equation were first non-dimensionalized. The transport equation was then integrated with the use of the boundary conditions. The resulting integral was solved by assuming a density profile such that the developing region was divided into a uniform core and a boundary layer. For the boundary layer profile a third order polynomial was selected of the form $R^* = 1 - (1 + d)\eta^2 + d\eta^3$ Where R^* is the ratio of dimensionless particle density to centerline particle density, $\eta = (\lambda^* - 1 + M) / M$, λ^* is the ratio of axial distance to tube radius, m is the ratio of the density boundary layer thickness to the radius of the tube, $1 - M\lambda^* \leq 1$ and d is an arbitrary constant which was determined so that the integral and auxiliary equations was satisfied when the flow was fully developed. The set of differential equations was solved numerically.

The results of this study showed that for any axial distance for both plug flow and Poiseuille flow, the deposition increased as the electrostatic charge parameter increased. In this analysis it was assumed that all particles which contacted the wall were completely absorbed.

3. LAMINAR FLOW OF PARTICLES IN A
PARALLEL-PLATE CHANNEL WITH ELECTROSTATIC CHARGE,
DIFFUSION, AND GRAVITATIONAL EFFECTS

3.1 General Description

A numerical method is presented to study the deposition of particles in suspension in a parallel-plate channel due to the effects of electrostatic charge and diffusion and that of charge and gravity in the direction of flow. A comparison is made in the deposition due to the effects of electrostatic charge and gravity with the deposition due to the effect of electrostatic charge alone and the range of charge effect for which the diffusive effect may be neglected is determined.

Also, the deposition of particles in a vertical channel due to the effects of electrostatic charge and gravity was studied using numerical analysis.

The Assumptions Used In This Analysis Are:

- (1) Incompressible, steady flow.
- (2) Two-dimensional, laminar flow
- (3) Negligible axial component of electric field intensity.
- (4) Negligible axial component of diffusive force.
- (5) Dilute suspension (density of fluid phase \gg particle concentration).

- (6) Fluid-particle interaction follows Stokes' Drag Law
 (F = inverse of the relaxation time for momentum transfer = $9\mu\bar{\rho}_p/2a^2$ where μ is the fluid viscosity, a is the particle radius and $\bar{\rho}_p$ is the particle density.
- (7) Particle to particle interaction is negligible.
- (8) Thickness of layer of deposit is much smaller than the channel width.
- (9) Negligible material density of the fluid phase as compared with the density of the particles in suspension.
- (10) Constant viscosity
- (11) No chemical reactions
- (12) No temperature change

Referring to Fig. 3.1, rectangular cartesian coordinates are utilized in this analysis. The x-axis is the centerline of the channel and the y-axis is in the orthogonal direction. u is the axial component of the fluid velocity, v is the component in the y-direction. The flow occurs between the two fixed channel walls spaced a distance $2h$ apart.

3.2 Governing Equations

a) Fluid Phase

$$\frac{\partial u}{\partial x} + \frac{\partial v}{\partial y} = 0 \quad \text{(Continuity Eq) (3-1)}$$

This may be expressed in integral form as

$$2 \int_0^h u dy = 2 u_0 h$$

$$u \frac{\partial u}{\partial x} + v \frac{\partial u}{\partial y} = -\frac{1}{\rho} \frac{dP}{dx} + \mu \frac{\partial^2 u}{\partial y^2} \quad \text{(N.S. Eq. of Motion (3-2) for Newtonian Fluid)}$$

b) Particulate Phase

$$\frac{\partial}{\partial x} (\rho_p u_p) + \frac{\partial}{\partial y} (\rho_p v_p) = 0 \quad \text{Continuity Eq. (3-3)}$$

$$\frac{\partial e_x}{\partial x} + \frac{\partial e_y}{\partial y} = \frac{\rho_p q}{\epsilon_0 m_p} \quad \text{Poisson's Eq. (3-4) for electric field}$$

Force
on a unit
charge
in x-direction

Electric
Field intensity

Combine Eq. (1) and (3)

$$u \frac{\partial \rho_p}{\partial x} + v \frac{\partial \rho_p}{\partial y} + \frac{\partial}{\partial x} [\rho_p (u_p - u)] + \frac{\partial}{\partial y} [\rho_p (v_p - v)] = 0$$

Simplify by letting

$$\rho_p (u_p - u) = (J_p)_x \quad \text{Mass Flux in x-direction}$$

$$\rho_p (v_p - v) = (J_p)_y \quad \text{Mass Flux in y-direction}$$

The above Eq. can be simplified to read

$$u \frac{\partial \rho_p}{\partial x} + v \frac{\partial \rho_p}{\partial y} = -\frac{\partial}{\partial x} (J_p)_x - \frac{\partial}{\partial y} (J_p)_y \quad (3-5)$$

Fick's law for mass transfer states that the mass flux equals the mass diffusivity times the mass concentration gradient.

Including the actions of the external electric field force and the effect of gravity we have

$$(J_p)_y = \left(\frac{q}{m_p} \right) \frac{\rho_p e_y}{F} - D \frac{\partial \rho_p}{\partial y}$$

$$(J_p)_x = \left(\frac{q}{m_p} \right) \frac{\rho_p e_x}{F} - D \frac{\partial \rho_p}{\partial x} - \rho_p v_g$$

Since an electrostatic field is a conservative field

$$\nabla \times \mathbf{e} = \frac{\partial e_x}{\partial y} - \frac{\partial e_y}{\partial x} = 0 \quad (3-6)$$

assuming that $\frac{y}{x} \sim \frac{h}{L} \sim \epsilon$ and $\epsilon \ll 1$ Eq. 3-6 gives $\frac{e_x}{e_y} \sim \epsilon$
 Thus, e_x is negligible when compared with e_y and the electrostatic force in the x-direction may be neglected.

The electric field force in the x-direction, the diffusive force in the x-direction, and the effect of gravity in the y-direction are assumed to be negligible compared with the other forces so that we have

$$-\frac{\partial(J_p)_x}{\partial x} - \frac{\partial(J_p)_y}{\partial y} = \frac{\partial}{\partial y} \left[\frac{q}{m_p} \frac{\rho_p e_y}{F} \right] + \frac{\partial}{\partial y} \left[D \frac{\partial \rho_p}{\partial y} \right] + \frac{\partial}{\partial x} \left[\rho_p v_g \right]$$

Substituting the above equation into Eq. 3-5, we get

$$u \frac{\partial \rho_p}{\partial x} + v \frac{\partial \rho_p}{\partial y} = - \frac{\partial}{\partial y} \left[\frac{q}{m_p} \frac{\rho_p e_y}{F} \right] + \frac{\partial}{\partial y} \left[D \frac{\partial \rho_p}{\partial y} \right] + \frac{\partial}{\partial x} \left[\rho_p v_g \right] \quad (3-7)$$

Eq. 3-7 is the steady state diffusion equation.

In Equation 3-7 the axial diffusive force has been neglected assuming that the Peclet number is high (> 50). Refer to Tau and Hsu [12].

Further, we assume $v = v_p = 0$ for all values of y .

Thus the equations which we wish to solve are

$$u \frac{\partial \rho_p}{\partial x} = - \frac{\partial}{\partial y} \left[\frac{q}{m_p} \frac{\rho_p e_y}{F} \right] + \frac{\partial}{\partial y} \left[D \frac{\partial \rho_p}{\partial y} \right] + \frac{\partial}{\partial x} \left[\rho_p v_g \right] \quad (3-8)$$

$$\frac{\partial e_y}{\partial y} = \frac{\rho_p q}{\epsilon_0 m_p} \quad (3-9)$$

3.3 Analysis for Diffusion and Electrostatic Charge

The Equation of diffusion which expresses the particle cloud concentration ρ_p in the flow stream is

$$u \frac{\partial \rho_p}{\partial x} = D \frac{\partial^2 \rho_p}{\partial y^2} - \frac{\partial}{\partial y} \left[\frac{q}{\mu_p} \frac{\rho_p e_y}{F} \right] \quad (3-10)$$

The electrostatic field intensity is governed by Poisson's Equation as given in Eq. 3-9.

The boundary conditions are

At $x = 0$ (inlet plane) for $0 \leq y \leq h$ $\rho_p = \rho_{p0}$ (uniform)

At $y = 0$ (centerline) for $x > 0$ $\frac{\partial \rho_p}{\partial y} = 0$ (symmetry)

At $y = 0$, $e_y = 0$ (centerline)

At $y = h$, (wall) for $x > 0$, $\rho_p = 0$ (for complete absorption)

Eq. (3-9) and Eq. (3-10) in dimensionless form (See Appendix A)

become

$$\frac{u \partial R}{\partial x^*} = \frac{\partial^2 R}{\partial Y^2} - E \frac{\partial R}{\partial Y} - \alpha R^2 \quad (3-11)$$

$$\frac{\partial E}{\partial Y} = +\alpha R \quad (3-12)$$

Where $X^* = \frac{X}{\rho}$, the diffusive Peclet number = β , electrostatic charge parameter = α , and other variables are as defined in the Nomenclature.

The only variable in these equations is α .

In non-dimensionalized form the boundary conditions are

At $X = 0$ (inlet plane) for $0 \leq Y \leq 1$ $R = 1$ (uniform)

At $Y = 0$ (centerline) for $X > 0$ $\frac{\partial R}{\partial Y} = 0$ (symmetry)

At $Y = 1$ (wall) for $X > 0$, $R = 0$ (complete absorption)

The velocity profile is considered either uniform ($U = 1.$) or parabolic flow ($U = 1.5 (1-Y^2)$).

Equations (3-11) and (3-12) are expressed in an implicit finite difference representation about $i + 1, j$ as follows. Refer to Hornbeck [3,29] and Quarmby [26] .

$$U_{i+1,j} \left[\frac{R_{i+1,j} - R_{i,j}}{\Delta X^*} \right] = \frac{R_{i+1,j+1} - 2R_{i+1,j} + R_{i+1,j-1}}{\Delta Y^2} - E_{i,j} \left[\frac{R_{i+1,j+1} - R_{i+1,j-1}}{2 \Delta Y} \right] - 4\alpha R_{i,j} [R_{i+1,j}] \quad (3-13)$$

$$\frac{E_{i+1,j+1} - E_{i+1,j}}{\Delta Y} = 4 \alpha R_{i+1,j} \quad (3-14)$$

Twenty-one mesh points across the flow from the centerline to the wall were used. Each increment in the Y- direction was maintained constant at $Y = 0.05$. The increments in the X- direction varied from $\Delta X^* = 0.00001$ to 0.001 such that convergence was achieved [26].

As Hornbeck [29] indicated, the implicit representation used in this solution can be shown to be stable for all mesh sizes. This is in contrast to the explicit representation which is restricted to small axial increments. The increments in the axial direction were taken small (.00001) to start and were increased as the solution proceeded. The selection of the step sizes were varied from large to small until consistent solutions were developed.

3.4 Analysis For Electrostatic Charge Only

When the electrostatic charge effect is very strong in comparison with the diffusion effect, one may neglect the diffusion term in Eq. (3-10).

$$\mu \frac{\partial P_P}{\partial x} = -\frac{\partial}{\partial y} \left[\frac{q}{\gamma_P} \frac{\rho_P e_y}{F} \right] \quad (3-15)$$

Similarly Eq. (3-9) may be rewritten

$$\frac{\partial e_y}{\partial y} = \frac{\rho_P q}{\epsilon_0 \gamma_P} \quad (3-9)$$

The boundary conditions are similar to those presented previously.

In dimensionless form (see Appendix A), Eq. (3-9) and (3-15)

become

$$U \frac{\partial R}{\partial \left(\frac{1+\alpha X}{\beta} \right)} = - \left(\frac{E}{1+\alpha} \right) \frac{\partial R}{\partial Y} - R^2$$

and

$$\left(\frac{1}{1+\alpha} \right) \frac{\partial E}{\partial Y} = R$$

or

$$U \frac{\partial R}{\partial X_1^*} = - E^* \frac{\partial R}{\partial Y} - R^2 \quad (3-16)$$

and

$$\frac{\partial E^*}{\partial Y} = R \quad (3-17)$$

Eq. (3-16) in conjunction with Eq. (3-17) can be solved numerically using an explicit finite difference representation about $i + 1, j$. (see Appendix C).

$$\begin{aligned} & \left[\Delta Y \right] R_{i+1, j}^2 + \left[U_{i+1, j} \cdot \frac{\Delta Y}{\Delta X_1^*} + E_{i, j}^* \right] R_{i+1, j} \\ & - \left[U_{i+1, j} \cdot \frac{\Delta Y}{\Delta X_1^*} \right] R_{i, j} - \left[E_{i, j}^* \right] R_{i+1, j-1} = 0 \end{aligned} \quad (3-18)$$

Eq. (3-18) can be explicitly solved for $R_{i+1,j}$

Having calculated $R_{i+1,j}$ the electrostatic field intensity may be calculated from Eq. (3-17) (see Appendix C) such that

$$E_{i+1,j+1}^* = R_{i+1,j} \Delta Y + E_{i+1,j}^* \quad (3-19)$$

For $0 \leq X_1^* \leq 0.04$, 81 mesh points were used across the flow from the centerline to the wall and ΔY was held constant at 0.0125.

For $X_1^* > 0.04$, 41 mesh points ($\Delta Y = 0.025$) were used. ΔX_1^* varied from 0.0001 to 0.01.

The mesh size has been established to assure the stability and convergence of the solution. Comparable mesh sizes have been used by previous investigators such as Hornbeck [29], and Chen [6]. Several trial runs were selected in this investigation before final step sizes were selected. Selected steps in the Y- direction were taken for $\Delta Y = .025, .050, \text{ and } 0.10$. The increment of 0.0125 was used as the initial step and later increased to 0.025.

When fine particles in suspension enter a channel a fraction of the particles will be deposited on the wall and the remainder continue in suspension. The fractional penetration at the corresponding axial distance from the entrance is expressed as

$$\int_0^1 URdY.$$

This may be integrated by using Simpson's Rule (see Appendix C).

By substituting Eq. (3-17) into Eq. (3-16), it can be shown that the closed form analytic solution for uniform flow is $R = 1/(1+X_1^*)$ which is also equal to the fraction of penetration. The distribution of R is, therefore, uniform across the flow and is a function of X_1^* alone. This result for plug flow is in agreement with the numerical analysis. (see Appendix C).

3.5 Analysis for Electrostatic Charge With Gravity in the Direction of Flow.

For this case a vertical channel is considered with gravity acting in the direction of flow as shown in Fig. 3.1.

The governing equations derived from equations (3-8) and (3-9) include both the charge effect and gravity are

$$u \frac{\partial \rho_p}{\partial x} = - \frac{\partial}{\partial y} \left[\frac{q}{m_p} \frac{\rho_p e_y}{F} \right] + \frac{\partial}{\partial x} \left[\rho_p v g \right] \quad (3-20)$$

$$\frac{\partial e_y}{\partial y} = \frac{\rho_p g}{\epsilon_0 m_p} \quad (3-9)$$

These equations may be non-dimensionalized into the following form (see Appendix B).

$$(S + U) \frac{\partial R}{\partial X_i^*} = - E^* \frac{\partial R}{\partial Y} - R^2 \quad (3-21)$$

$$\frac{\partial E^*}{\partial Y} = R \quad (3-22)$$

Where $S = \frac{v_g}{u_0}$ is the ratio of the terminal velocity of the particle in a still air to the mean velocity.

For vertical channel flow, the particles are assumed to maintain a velocity of $u + v_g$ throughout the flow.

The boundary conditions are as described for the previous cases.

The fractional penetration at the corresponding axial distance

from the entrance is expressed as

$$\frac{\text{Particles continuing in suspension}}{\text{Particles entering channel}} = \frac{\int_0^h (u + v_g) \rho_p dy}{\int_0^h (u_0 + v_g) \rho_p dy}$$

Where $(u + v_g)$ = particle velocity

This equation may be non-dimensionalized into

$$\frac{\int (U + S) R dY}{1 + S} \quad (3-23)$$

The fractional deposition can be found by (1 - fractional penetration).

Equation (3-21) together with (3-22) can be solved numerically. These equations may be expressed in an explicit finite difference form about $i+1, j$ (see Appendix C) as follows:

$$\left(S + U_{i+1, j} \right) \frac{R_{i+1, j} - R_{i, j}}{\Delta X_1^*} = - E_{i, j}^* \cdot \frac{R_{i+1, j} - R_{i+1, j-1}}{\Delta Y} - \left(R_{i+1, j} \right)^2$$

Using the same method as in the previous case, eighty-one rectangular mesh points were selected at the entrance. The increments in the Y- direction were held constant at $\Delta Y = 0.0125$. The eighty-one mesh points were reduced to forty-one beyond the axial distance of X_1^* equal to 0.04 and the Y increment was increased to $\Delta Y = 0.025$.

In the axial direction the increments varied from $\Delta X_1^* = 0.0001$ to 0.01. The solution was determined explicitly.

3.6 Results and Discussion

The deposition of fine particles in channel flow has been studied for three cases. These involved the effects of

3.6.1 Diffusion and electrostatic charge,

3.6.2 Electrostatic charge only.

3.6.3 Electrostatic charge and gravity in the direction of flow.

These cases were studied with velocity profiles of uniform flow and of parabolic flow.

Consider Case (1) involving diffusion and electrostatic charge with

a uniform velocity profile. Solving Equations (3-11) and (3-12) using an implicit finite difference method for any axial distance X ($.001 \ll X \ll 100.$), where X is the ratio of axial distance to the half width of the channel, the deposition was found to increase with increasing electrostatic charge effect. The results are shown in Fig. 3.3 for the range of 0.0, 2.5, 5.0, 10.0, 50.0 and 100. Introducing a new dimensionless parameter of $4\alpha X/\beta$ where α and β are the electrostatic charge and diffusion parameters respectively, the results are plotted in Fig. 3.4. By varying this electrostatic charge parameter (2.5, 10.0, 100.0) it was found that for any dimensionless distance $4\alpha X/\beta$ the deposition increased as the electrostatic charge parameter decreased. The results are shown with an enlarged Detail insert. It is noted in comparing Fig. 3.3 and Fig. 3.4 that the new parameter has presented a compact set of curves and the results for $\alpha = 5.0$ and $\alpha = 50.0$ have been omitted only for clarity. Also, for comparison, a curve is plotted in Fig. 3.4 for the case where the diffusion term in Equation (3-12) is neglected leaving only the electrostatic charge. This curve is identified as $\alpha \rightarrow \infty$. As indicated in Fig. 3.4, the curves show α increasing and approaching a limit of negligible diffusion. From these curves it can be seen that when $\alpha > 50$, the diffusion term may be neglected and the solution to Equations (3-11) and (3-12) may be based on the electrostatic charge only.

Similar results were found for this same case involving diffusion and electrostatic charge using a parabolic velocity profile. Referring to Fig. 3.5 the deposition increased as the electrostatic charge effect

increased. The range was varied with $\alpha = 0.0, 2.5, 5.0, 10.0, 50.0$ and 100. as for the uniform velocity. It is noted however, that for any axial distance the values of deposition are less for parabolic flow than for uniform flow for the corresponding curves of electrostatic charge. This is attributed to fully developed flow. Referring to Fig. 3.6 the values for the deposition were then plotted against the same parameter $4 \alpha X / \beta$ and these curves were found to be even closer together at any value of $4 \alpha X / \beta$ for the various selected values of electrostatic charge. For values of $4 \alpha X / \beta$ up to about 8.0 the curves $\alpha \geq 10$. are not distinguishable. As in the case for uniform flow we see that when the electrostatic charge is greater than 50 the diffusion term may be neglected and the solution may be considered to be dependent on the electrostatic charge only.

Next, consider the Case (2) involving the deposition due to electrostatic charge only. Equations (3-16) and (3-17) were solved using the explicit method. The results for uniform flow are shown in Fig. 3.4 while the results for parabolic flow are shown in Fig. 3.6. In each Figure these curves are identified as $\alpha \rightarrow \infty$. This is the curve where $\alpha \rightarrow \infty$ when both electrostatic charge and diffusion are considered and where the diffusion is negligible compared with effect of the electrostatic charge.

Finally, Case (3) involves electrostatic charge and gravity in the direction of flow. Equation (3-21) with Equation (3-22) was solved explicitly. For the case of uniform flow it was found by introducing an axial distance parameter $X_2^* = \frac{X_1^*}{(S+1)}$ that Equation (3-21) may be reduced

to a form similar to Equation (3-16) where the solution is simply

$R = \frac{1}{(1 + X_2^*)}$. This result is plotted in Fig. 3.7. It should be noted that in this case there is only one curve for all variable δ .

The deposition determined from the solution of Equation (3-21) was plotted with a dimensionless axial distance parameter of $4 \propto X / (\delta + 1)\beta$ and the results are shown in Fig. 3.7. In this case a new parameter $\delta = v_g/u_o$, the ratio of terminal particle velocity to mean velocity, is introduced. The curves show for any dimensionless axial distance $4 \propto X / (\delta + 1)\beta$, as δ increases (0.0, 1.0, 10.0) the deposition increases. The curves also show that for any dimensionless axial distance, as δ increases the differences in the values for the deposition decrease. Note that this statement is based on the dimensionless axial distance $4 \propto X / (\delta + 1)\beta$. In actual channel flow the deposition at any axial distance X will decrease with increasing δ in both uniform and parabolic flow.

It may be seen that as δ increases the deposition approaches the curve for uniform flow. In practical cases the value of δ will be much less than 1. Calculations have been made for $0 < \delta < 1$ and these curves fall between $\delta = 0$ and $\delta = 1$. As seen from the curves in Fig. 3.7 for values of $\delta > 10$ the velocity profile of the fluid has negligible effect on the deposition. This is as expected since at the high velocity ratios the particle velocity profile ($u + v_g$) is relatively uniform (10.0 u near the wall and 11.0 u at the centerline). The compactness of this set of curves is due to the choice of the coordinate system and is, therefore, a distinct advantage of the selected dimensionless axial distance.

4. THE EFFECT OF THE TERMINAL VELOCITY AND THE VELOCITY DEVELOPMENT ON THE DEPOSITION IN A VERTICAL TUBE

4.1 General Description

When fine particles enter a vertical tube, particles are deposited on the wall due to diffusion. This study is a numerical analysis to determine the effects on the deposition due to the velocity ratio \mathcal{S} for various Schmidt numbers. The velocity ratio is the ratio of the gravity flow parameter ($v_g r_o / D$) to the diffusive Peclet number ($u_o r_o / D$), while the Schmidt number is the ratio of the diffusive Peclet number to the Reynolds number ($u_o r_o / \nu$). The influence of the velocity ratio is used to establish the conditions which will determine when the deposition is not greatly influenced by the velocity profile so that the problem may be simplified by assuming the flow to be uniform.

Also, this study will determine the effect on the deposition of varying the velocity ratio \mathcal{S} with a new axial parameter $\frac{x/\beta}{\mathcal{S}+1}$ for Poiseuille flow and for uniform flow.

The assumptions used in this analysis are the same as those used in Chapter 3 in the analysis for flow in a parallel-plate channel. The effect of electrostatic charge is not included.

When a suspended solid particle enters a vertical tube at the same velocity of the fluid, the particle will experience gravitational acceleration and after a very short period of relaxation it will reach its steady axial velocity of $u + v_g$ so long as the fluid velocity remains

constant. In this analysis it is assumed that each particle enters the tube at a uniform velocity of $u_0 + v_g$, where u_0 is the uniform inlet velocity of the fluid, and that the particle maintains its velocity at $u + v_g$ thereafter.

This assumption is more realistic than assuming an inlet velocity of u_0 for the particle since in experiment a short piece of tube is always present between the aerosol generator and the test tube. Further, this assumption is reasonable since the fluid velocity develops gradually in the hydrodynamic entrance region.

4.2 Governing Equations

In the entrance region the governing equations are

a) Fluid Phase

$$\frac{\partial u}{\partial x} + \frac{1}{r} \frac{\partial (rv)}{\partial r} = 0 \quad \text{Continuity Eq. (4-1)}$$

$$\mu \frac{\partial u}{\partial x} + v \frac{\partial u}{\partial r} = -\frac{1}{\rho} \frac{\partial P}{\partial x} + \frac{\mu}{\rho r} \frac{\partial}{\partial r} \left(r \frac{\partial u}{\partial r} \right) + \frac{\mu}{\rho r^2} \frac{\partial^2 u}{\partial x^2} \quad (4-2)$$

N.S.Eq. of motion for Newtonian fluid.

b) Particulate Phase

$$\frac{\partial}{\partial x} (\rho_p u_p) + \frac{1}{r} \frac{\partial}{\partial r} (r \rho_p v_p) = 0 \quad \text{Continuity Eq. (4-3)}$$

The procedure used in solving these equations is similar to that used in Chapter 3, and the diffusion equation for the particulate phase neglecting the axial diffusion term is given as

$$u \frac{\partial \rho_p}{\partial x} + v \frac{\partial \rho_p}{\partial r} = D \frac{1}{r} \frac{\partial}{\partial r} \left(r \frac{\partial \rho_p}{\partial r} \right) - \frac{\partial}{\partial x} (v_g \rho_p) \quad (4-4)$$

Where x is the axial coordinate placed along the centerline of the vertical tube, r is the radial distance, u and v the velocities in the x and r directions respectively, ρ_p the particle density, D the particle diffusivity and v_g the terminal velocity of the particles.

Referring to Appendix B for dimensionless quantities and parameters the diffusion equation in dimensionless form becomes

$$(\delta + U) \frac{\partial R}{\partial X} + \beta V \frac{\partial R}{\partial r^*} = \frac{1}{r^*} \frac{\partial}{\partial r^*} \left(r^* \frac{\partial R}{\partial r^*} \right) \quad (4-5)$$

Where δ = velocity ratio

U = dimensionless axial velocity

R = dimensionless particle concentration

X = dimensionless axial distance

V = dimensionless radial velocity

r^* = dimensionless radial distance from axis

β = diffusive Peclet number

The boundary conditions are

At $X = 0$ (inlet plane), for $0 \leq r^* \leq 1$ $R = 1$ (Uniform)

At $r^* = 0$ (axis) for $X > 0$ $\frac{\partial R}{\partial r^*} = 0$ (Symmetry)

At $r^* = 1$ (wall) for $X > 0$ $R = 0$ (Complete absorption)

Equation 4-5 in conjunction with the continuity equation 4-1 may be written as

$$\frac{\partial}{\partial X} \left[(S + U) R r^* \right] + \frac{\partial}{\partial r^*} (\beta V R r^*) = \frac{\partial}{\partial r^*} \left(r^* \frac{\partial R}{\partial r^*} \right) \quad (4-6)$$

In this analysis the radial velocity V is assumed to be negligible, $V = 0$.

The velocity profile is approximated as follows

For uniform flow, $U = 1$

For developing flow, $U = U_c (1.0 - \gamma^N)$

where $U_c = (1.0 + 2.0/N)$

if $0 \ll X \ll 0.25 \text{ Re}$

$N = 0.645 (X/\text{Re})^{-0.497} + 2.10 (X/\text{Re})^{0.765}$

if $X > 0.25 \text{ Re}$

$N = 2.0$

For parabolic flow, $U = 2.0 (1 - \gamma^2)$

4.3 Analysis of Solution

In this analysis the field flow is divided into small control volumes. A typical interior control volume with a radial increment of S_3 and an axial increment of H as shown in Fig. 4.1 is analyzed as follows.

Integrating Eq. 4-6 with respect to r^* from $r^* = b_2$ to $r^* = b_3$ gives an approximate finite difference expression.

$$\begin{aligned} & \lambda_3^* S_3 (\delta + U_{2,3}) R_{2,3} - \lambda_3^* S_3 (\delta + U_{1,3}) R_{1,3} \\ & + \beta H b_3 V_3 \bar{R}_3 - \beta H b_2 V_2 \bar{R}_2 \\ & = \frac{H b_3}{S_3 + S_4} (R_{2,4} - R_{2,3} + R_{1,4} - R_{1,3}) \\ & - \frac{H b_2}{S_2 + S_3} (R_{2,3} - R_{2,2} + R_{1,3} - R_{1,2}) \end{aligned} \quad (4-7)$$

Where \bar{R}_3 and \bar{R}_2 are the average values of R along the control surface b_3 and b_2 respectively. This average particle density may be obtained by linear interpolation. For example,

$$\bar{R}_3 = \frac{1}{2} \left[R_{2,4} + R_{1,4} + (R_{2,3} - R_{2,4} + R_{1,3} - R_{1,4}) \frac{S_4}{S_3 + S_4} \right] \quad (4-8)$$

Similar control volume approach was used in this analysis for the control volume enclosing the centerline and that at the wall. The radial increment for each control volume S_j was chosen such that $S_j/S_{j-1} = 0.91523$, $S_1 = 0.107637$, and $S_{20} = 0.02$. The flow field was discretized into 21 mesh points in the radial direction and the increments in the X - direction varied gradually from 10^{-5} near the inlet

plane of the tube to 0.002 near the end of the tube where the fractional penetration becomes less than 0.02.

Equation (4-6) may be expressed in an implicit finite difference representation about $i + 1, j$ as follows (see Appendix C).

$$\begin{aligned}
& - \left[\frac{H b_{j-1}}{S_{j-1} + S_j} + \frac{\beta H b_{j-1} V_{j-1} S_j}{2(S_{j-1} + S_j)} \right] R_{i+1, j-1} \\
& + \left[\lambda_j^* S_j (S + U_{i+1, j}) + \frac{\beta H b_j V_j S_{j+1}}{2(S_j + S_{j+1})} - \frac{\beta H b_{j-1} V_{j-1}}{2} \right. \\
& + \left. \frac{\beta H b_{j-1} V_{j-1} S_j}{2(S_{j-1} + S_j)} + \frac{H b_j}{(S_j + S_{j+1})} + \frac{H b_{j-1}}{(S_{j-1} + S_j)} \right] R_{i+1, j} \\
& + \left[\frac{\beta H b_j V_j}{2} - \frac{\beta H b_j V_j S_{j+1}}{2(S_j + S_{j+1})} - \frac{H b_j}{(S_j + S_{j+1})} \right] R_{i+1, j+1} \\
& = \left[\frac{H b_{j-1}}{(S_{j-1} + S_j)} + \frac{\beta H b_{j-1} V_{j-1} S_j}{2(S_{j-1} + S_j)} \right] R_{i, j-1} \\
& + \left[\lambda_j^* S_j (S + U_{i, j}) + \frac{\beta H b_{j-1} V_{j-1}}{2} - \frac{\beta H b_{j-1} V_{j-1} S_j}{2(S_{j-1} + S_j)} - \frac{H b_j}{(S_j + S_{j+1})} \right. \\
& - \left. \frac{\beta H b_j V_j S_{j+1}}{2(S_j + S_{j+1})} - \frac{H b_{j-1}}{(S_{j-1} + S_j)} \right] R_{i, j} \\
& + \left[- \frac{\beta H b_j V_j}{2} + \frac{\beta H b_j V_j S_{j+1}}{2(S_j + S_{j+1})} + \frac{H b_j}{(S_j + S_{j+1})} \right] R_{i, j+1} \quad (4-9)
\end{aligned}$$

The fractional penetration at an axial distance corresponding with the solution of Eq. (4-9) is expressed as

$$1 - \frac{2 \int (\xi + U) R \lambda^* d\lambda^*}{(\xi + 1)} \quad (4-10)$$

In this analysis $\beta = 100$ and $Re = 10,100$ and $1,000$ corresponding to Schmidt Number $Sc = \beta / Re = 10, 1$ and 0.1 were employed.

4.4 Results and Discussion

The velocity ratio $\xi = \frac{v_g}{u_0}$ is the ratio of the gravity flow parameter to the diffusive Peclet Number, which is the ratio of the gravity force to the inertia force. The Schmidt Number $Sc = \beta / Re$ is the ratio of the viscous forces to the diffusive forces. The effect of the velocity ratio ξ and the Schmidt Number Sc over the axial distance $0 < \frac{X}{\beta} < 1$ is shown in Fig. 4.3. The fractional penetration for developing flow (e.g. $Sc = 1$ and $\xi = 1$) is very close to that for uniform flow (when $Sc = 0$) near the inlet plane of the tube $\frac{X}{\beta} < .001$. As the flow becomes more fully developed the penetration approaches that of Poiseuille flow (when $Sc \rightarrow \infty$). This characteristic is also observed in simple diffusion (i.e. flow without gravitational effect). As expected the penetration increases for a given axial distance as the velocity ratio v_g/u_0 is increased. From Equation 4-6 it is easily seen that for plug flow $U = 1$ a new dimensionless distance $X(1 + \xi)$ can be defined such that the governing equation reduces to that of the simple diffusion equation for the plug flow which has been solved by many investigators [4, 14, 15, 16]. This dimensionless distance is used in Fig. 4.4. Two

Two penetration curves ($v_g/u_o = 1.0$ and 10.0) are also shown. The penetration curve for $v_g/u_o = 10.$ for Poiseuille flow was found to almost coincide with the curve for plug flow. In other words, when the terminal velocity is about 10 times the fluid velocity, the effect of the velocity development becomes insignificant. This is as expected since at high velocities the velocity profile for the particle phase is relatively flat with v_g at the wall, and the flow is similar to high slip velocity profile. The dimensionless axial distance used in Fig. 4.4 is desirable due to the fact that the penetration for the plug and Poiseuille flow with no gravity effect is well defined and readily available [2, 9].

The deposition of suspensions in the entrance region of a parallel-plate vertical channel based on the fractional penetration was also investigated and are shown in Fig. 4.5 and Fig. 4.6.

Experimental measurements have been made by Wong Kittirock [28] for the flow of particles in a vertical tube under the influence of electrostatic charge. See Figure 3.8. The results show the effect of the dimensionless axial distance $4\alpha X/\xi$ on the fraction of deposition for a concentration range from 35 to 50 pt./cc. This is for a uniform velocity profile. The results of fully developed flow were close to those for uniform flow. While test data is not available for channel flow these results show close agreement with the solution for channel flow. Values of the fraction of deposition at $4\alpha X/\xi = 0, .05, .10,$ and $.15$ were compared and found to confirm the corresponding deposition values of $0.0, .05, .09,$ and $.13.$

5. CONCLUSIONS

This investigation was made to determine the effect on the deposition of fine particles in a vertical channel and in a vertical tube due to the influence of electrostatic charge, diffusion and gravity acting in the direction of flow.

The conclusions reached are as follows:

For a parallel-plate channel

1. Considering the influence of diffusion and electrostatic charge, the deposition was found to increase with increasing electrostatic charge.
2. Considering diffusion and electrostatic charge, for any selected axial distance along the channel and for the same electrostatic charge, the deposition was greater for uniform flow than for parabolic flow.
3. Considering diffusion and electrostatic charge, for uniform flow and for a selected axial distance, curves plotted showing deposition versus axial distance resulted in a wide band of deposition values as the electrostatic charge was varied from 0.0 to 100. When a new dimensionless distance $4 \alpha X/\beta$ was selected, the deposition was found to decrease as the electrostatic charge parameter α increased and also the wide band of curves became more closely packed. The result is that if the electrostatic charge parameter

α is greater than 50. then the diffusion term may be neglected and the deposition may be determined from the electrostatic charge only.

4. Similar results were found using a parabolic velocity profile and with the new dimensionless distance $4\alpha X/\beta$ the curves are packed even more closely together for the range of selected values of electrostatic charge. For parabolic flow it may also be concluded that if the electrostatic charge parameter α is greater than 50. then the diffusive term may be neglected.
5. When the diffusive effect is neglected and only the effects of electrostatic charge and gravity are considered, then for a given axial distance X the deposition decreases as the gravity effect increases. As the velocity ratio ξ exceeds 1. the effect of the velocity profile on the deposition decreases with the curve approaching that of uniform flow.
6. The analysis for flow in a vertical parallel plate channel considered only uniform and parabolic flows. It is expected that the deposition will fall between these for developing flow.
7. For a vertical tube, the fractional penetration near the inlet of the tube ($X < 0.001$) was found to be very close to that for uniform flow. As the flow becomes more fully developed ($X > 1$), the penetration was found to approach that for Poiseuille flow.

8. For a vertical tube, for any given axial distance and for any velocity ratio $\xi = v_g/u_0$, the penetration increases as the Schmidt Number Sc increases.
9. For a vertical tube, for any given axial distance and for any value of the Schmidt Number, the penetration increases as the velocity ratio increases.
10. For a vertical parallel-plate channel the effects of the velocity ratio and that of the Schmidt Number are similar to that of the vertical tube with the exception that for corresponding distances the penetration for the parallel-plate channel is greater than that for the vertical tube.
11. For a vertical tube with a uniform velocity profile a new axial dimensionless distance $X/(1+\xi)$ was defined. The governing equation included the effects of both diffusion and gravity but by introducing this new parameter the equation was reduced to that of the simple diffusion equation.
12. For a vertical tube with a parabolic velocity profile, curves were plotted showing the penetration along the axial distance for a range of velocity ratios of 0.1 to 10. It was found that when the velocity ratio is about 10. (i.e. terminal velocity = 10 times fluid velocity) that the effect of the velocity ratio is insignificant and the penetration curve for parabolic flow almost coincides with that for uniform flow.

13. For a vertical parallel-plate channel the curves are similar to those for a vertical tube except that for any selected axial distance and for any comparable velocity ratio the deposition is greater for flow in a circular tube.
14. For a vertical parallel-plate channel the use of the axial parameter $\frac{x/\rho}{1 + \delta}$ results in a more compact set of curves than for the circular tube.

6. RECOMMENDATIONS FOR FUTURE STUDY

This investigation considered the hydrodynamics of a system of solid particles of uniform size and mass in a fluid suspension acting in a vertical conduit. Such analysis is of value and has practical application in the transport of waste products from various production processes. It also has application in human circulatory systems. Further study should include an extension of some of the limitations and restrictions imposed upon this investigation such as the use of the vertical channel or tube with flow in the direction of gravity. Further investigation may include inclining the conduit.

Also, consideration may be given to the condition where more than one size and mass of solid particle may be suspended in the fluid. Such application would be useful in internal combustion engine exhaust and also industrial dust collectors which frequently operate with multiple types of solids.

This dissertation was based on assumptions which provided that the flow is relatively slow. At higher velocities the boundary layer analysis requires that variations in density and temperature must be taken into account. The governing equations would have to be adjusted to account for compressibility of the fluid and additional equations would be needed such as an equation of state and an equation of conservation of energy in the boundary layer.

REFERENCES

1. Taulbee, D. B., "The Effect of Diffusion on the Settling of Aerosol Particles in Flow in a Parallel-Plate Channel", J. Aerosol Sci., Vol. 10, 1979, pp. 95-102.
2. Ingham, D. B., "Diffusion of Aerosols From a Stream Flowing Through a Cylindrical Tube", J. Aerosol Sci., Vol. 6, 1975, pp. 125-132.
3. Hornbeck, R. W., "Laminar Flow in the Entrance Region of a Pipe", Appl. Sci., Res., Sect. A., Vol. 13 pp. 224-232, 1964.
4. Ingham, D. B., "Deposition of Charged Particles Near the Entrance of a Cylindrical Tube", J. Aerosol Sci., Vol. 11, 1979, pp. 47-52.
5. Chen, R. Y., "Diffusive Deposition of Particles in a Short Channel", Powder Technology, 16 (1977), pp. 131-135.
6. Chen, R. Y. and Korjack, T. A., "Depositions of Suspensions in the Entrance Region of a Vertical Channel", Power Technology, 25 (1980) pp. 121-124.
7. Ingham, D. B., "Diffusion and Sedimentation of Aerosol Particles from Poiseuille Flow in Rectangular Tubes", J. Aerosol Sci., 7 (1976), pp. 13-18.
8. Chen, R. Y., "Deposition of Aerosol Particles in a Channel due to Diffusion and Electric Charge", J. Aerosol Sci., Vol. 9, 1978, pp. 253-260.
9. Chen, R. Y., "Deposition of Charged Particles in Tubes", J. Aerosol Sci., Vol. 9, 1978, pp. 449-453.
10. Ingham, D. B., "Diffusion and Sedimentation of Aerosol Particles from Poiseuille Flow in Rectangular Tubes", J. Aerosol Sci., Vol. 7, 1976, pp. 13-20.
11. Ingham, D. B., "Simultaneous Diffusion and Sedimentation of Aerosol Particles in Rectangular Tubes", J. Aerosol Sci., Vol. 7, 1976, pp. 373-380.
12. Tau, S. W. and Hsu, C. J., "Diffusion of Aerosols in Laminar Flow in a Cylindrical Tube", J. Aerosol Sci., Vol. 2, 1971, pp. 117-124.
13. Taulbee, D. B. and Yu, C. P., J. Aerosol Sci. Vol. 6, 1975, pp. 433-438.

14. Davies, C. N., "Diffusion and Sedimentation of Aerosol Particles from Poiseuille Flow in Pipes", J. Aerosol Sci., Vol. 4, 1973, pp. 317-322.
15. Gormley, P. and Kennedy, M., Proc. R. Ir. Acad., 1949, p. 163.
16. Thomas, J. W., 1967, Sump. Proc. Assessment of Airborn Radioactivity, pp. 701-712, Int. Atomic Energy Agency, Vienna.
17. Smutek, M., J. Aerosol Sci., 1972. Vol. 3, p. 337.
18. Campbell, W. D. and Slattery, J. C., "Flow in the Entrance of a Tube", ASME Paper No. 62, Hyd-6.
19. Longhaar, H. L., J. Appl. Mech., 9, Trans. Amer.Soc. Mech. Engrs., 64, 1942, A55.
20. Fuchs, N. A., "Mechanics of Aerosols", Pergamon Press, 1964.
21. Comparin, R. A., Chen, R. Y., and Eldighidy, S. M., "Deposition of Suspensions in Laminar Flow", Dept. of the Army, Contract DAAG 39-75-6-0059, HDL Proj. 302431, 1975, pp. 1-177.
22. Schlichting, H., "Boundary Layer Theory", McGraw-Hill Book Company, 6th Edition, 1968, Chapter IV and Chapter VII.
23. Carslaw, H. S. and Jaeger, J. C., "Conduction of Heat in Solids", Oxford University Press, London, 2nd Edition, 1959, p. 101.
24. Gupta, R. C., "Flow Development in the Hydrodynamic Entrance Region of a Flat Duct", AI Ch E. J., 11, 1965, p. 1149.
25. De Marcus, W. and Thomas, J., "Theory of a Diffusion Battery", USAEC ORDNL - 1413, 1952.
26. Quarmby, A., "A Finite Difference Analysis of Developing Slip Flow", Appl. Sci. Res., Vol. 19, 1968, pp. 18-33.
27. Davies, C. N., Aerosol Sci., Academic Press, London and New York, 1966, Chapter XII.
28. Wongkittirock, W., "The Effect of Electrostatic Charge on the Deposition of Suspensions Flow", Masters Thesis, 1980, N.J.I.T.
29. Hornbeck, R. W., "Numerical Methods", Quantum Publishers, Inc., N. Y., 1975, Chapter 11.
30. Bodoia, J. R. and Osterle, J. F., "Finite Difference Analysis of Plane Poiseuille and Couette Flow Developments", Appl. Sci., Res., Sect. A, Vol. 10, 1961, pp. 265-276.

APPENDIX ADIMENSIONLESS QUANTITIES AND PARAMETERS1. Dimensionless Quantities and Parameters

$$R = \frac{\rho_p}{\rho_{p0}}$$

$$U = \frac{u}{u_0}$$

$$V = \frac{v}{u_0}$$

$$X = \frac{x}{h}$$

$$Y = \frac{y}{h}$$

$$E_x = \left(\frac{q}{m_p} \frac{h}{FD} \right) e_x$$

$$E_y = \left(\frac{q}{m_p} \frac{h}{FD} \right) e_y$$

$$\alpha = \left(\frac{\rho_{p0}}{4\epsilon_0} \right) \left(\frac{q}{m_p} \right)^2 \left(\frac{h^2}{FD} \right)$$

$$\beta = \left(\frac{u_0 h}{D} \right)$$

$$Re = \left(\frac{u_0 h}{\nu} \right)$$

$$Sc = \frac{\beta}{Re} = \frac{\frac{u_0 h}{D}}{\frac{u_0 h}{\nu}} = \frac{\nu}{D}$$

2. Additional dimensionless quantities for vertical tube

$$X = \frac{x}{\beta \lambda_0}$$

$$r^* = \frac{r}{r_0}$$

$$\beta = \frac{u_0 \lambda_0}{D}$$

$$\eta = \frac{v_g \lambda_0}{D}$$

$$Re = \frac{u_0 \lambda_0}{\nu}$$

$$S = \frac{\eta}{\beta} = \frac{v_g}{u_0}$$

3. Physical meaning of parameters

$$Re = \frac{u_0 h}{\nu} \quad \text{Reynolds Number}$$

ratio of the inertia forces to the viscous forces.

$$\beta = \frac{u_0 h}{D} \quad \text{Diffusive Peclet Number}$$

ratio of the inertia forces to the diffusive forces of the particles.

$$\eta = \frac{v_g h}{D} \quad \text{Gravity Flow Parameter}$$

ratio of the gravity force to the diffusive force of the particles

$$\alpha = \left(\frac{\rho \rho_0}{4 \epsilon_0} \right) \left(\frac{q}{m_p} \right)^2 \left(\frac{h^2}{FD} \right) \quad \text{Electrostatic Charge Parameter}$$

ratio of the forces electrostatic charge to diffusion.

$$Sc = \frac{\beta}{Re} = \frac{\nu}{D} \quad \text{Schmidt Number}$$

ratio of the viscous forces to the diffusive force of the particles.

APPENDIX B

1. Case of channel flow considering diffusion and electrostatic charge effects.

$$u \frac{\partial p_p}{\partial x} = D \frac{\partial^2 p_p}{\partial y^2} - \frac{\partial}{\partial y} \left[\frac{q}{m_p} \frac{p_p e_y}{F} \right] \quad (3-11)$$

$$\frac{\partial e_y}{\partial y} = \frac{p_p q}{\epsilon_0 m_p} \quad (3-10)$$

Using the dimensionless quantities in Appendix A for Eq. 3-11.

$$u \frac{\partial p_p}{\partial x} = \frac{u_0 U p_{p0}}{h} \frac{\partial R}{\partial X}$$

$$D \frac{\partial^2 p_p}{\partial y^2} = D \frac{\partial}{\partial y} \left(\frac{\partial p_p}{\partial y} \right) = D \frac{p_{p0}}{h^2} \frac{\partial^2 R}{\partial Y^2}$$

$$-\left(\frac{q}{m_p F} \right) \frac{\partial e_y}{\partial y} = -\frac{q p_{p0} R}{m_p F} \frac{\partial E}{\left(\frac{q}{m_p} \right) \left(\frac{h^2}{FD} \right) \partial Y} = -\frac{D p_{p0}}{h^2} (4\alpha R^2)$$

$$-\left(\frac{q e_y}{m_p F} \right) \frac{\partial p_p}{\partial y} = -\left(\frac{q}{m_p F} \right) \left(\frac{m_p}{q} \right) \left(\frac{FD}{h} \right) \frac{E p_{p0}}{h} \frac{\partial R}{\partial Y} = -\frac{D p_{p0} E}{h^2} \frac{\partial R}{\partial Y}$$

Let

$$\frac{u_0 U p_{p0}}{h} \frac{\partial R}{\partial X} = \left(\frac{D p_{p0}}{h^2} \right) \frac{\partial^2 R}{\partial Y^2} - \left(\frac{D p_{p0}}{h^2} \right) 4\alpha R^2 - \left(\frac{D p_{p0} E}{h^2} \right) \frac{\partial R}{\partial Y}$$

$$\beta = \frac{u_0 h}{D}$$

$$U \frac{\partial R}{\partial \left(\frac{X}{\beta}\right)} = \frac{\partial^2 R}{\partial Y^2} - E \frac{\partial R}{\partial Y} - 4\alpha R^2$$

$$U \frac{\partial R}{\partial X^*} = \frac{\partial^2 R}{\partial Y^2} - E \frac{\partial R}{\partial Y} - 4\alpha R^2 \quad (3-12)$$

Where $X^* = \left(\frac{X}{\beta}\right)$

For Eq. 3-10

$$\frac{\partial E_Y}{\partial Y} = \frac{m_p F D}{q h^2} \frac{\partial E_Y}{\partial Y}$$

$$\frac{p p q}{E_0 m_p} = \frac{p p_0 R q}{E_0 m_p}$$

$$\frac{m_p F D \partial E_Y}{q h^2 \partial Y} = \frac{p p_0 R q}{E_0 m_p}$$

$$\frac{\partial E_Y}{\partial Y} = 4 \left[\frac{p p_0}{4 E_0} \left(\frac{q}{m_p}\right)^2 \frac{h^2}{F D} \right] R$$

$$\alpha = \left[\frac{p p_0}{4 E_0} \left(\frac{q}{m_p}\right)^2 \frac{h^2}{F D} \right]$$

$$\frac{\partial E_Y}{\partial Y} = 4\alpha R \quad (3-13)$$

2. Case of channel flow considering electrostatic charge effect only.

$$u \frac{\partial p_p}{\partial x} = - \frac{\partial}{\partial y} \left[\frac{q}{\mu_p} \frac{\rho_p e_y}{F} \right] \quad (3-14)$$

$$\frac{\partial e_y}{\partial y} = \frac{\rho_p q}{\epsilon_0 \mu_p} \quad (3-15)$$

Using the dimensionless quantities in Appendix A and following the same procedure as in case 1, these equations may be non-dimensionalized to the following

$$U \frac{\partial R}{\partial \left(\frac{4\alpha x}{\beta} \right)} = - \left(\frac{E}{4\alpha} \right) \frac{\partial R}{\partial Y} - R^2$$

$$\left(\frac{1}{4\alpha} \right) \frac{\partial E}{\partial Y} = R$$

or,

$$U \frac{\partial R}{\partial x_1^*} = - E^* \frac{\partial R}{\partial Y} - R^2 \quad (3-16)$$

$$\frac{\partial E^*}{\partial Y} = R \quad (3-17)$$

Where $x_1^* = \frac{4\alpha x}{\beta}$ and $E^* = \frac{E}{4\alpha}$

3. Case of channel flow considering charge effect with gravity.

$$u \frac{\partial p_p}{\partial x} = - \frac{\partial}{\partial y} \left[\frac{q}{\mu_p} \frac{\rho_p e_y}{F} \right] + \frac{\partial}{\partial x} \left[\rho_p v_g \right] \quad (3-20)$$

$$\frac{\partial e_y}{\partial y} = \frac{\rho_p q}{\epsilon_0 \mu_p} \quad (3-15)$$

Using the dimensionless quantities in Appendix A Eq. 3-20 may be non-dimensionalized in the following form.

$$\frac{\mu_0 U \rho \rho_0}{h} \frac{\partial R}{\partial X} = - \left(\frac{D \rho \rho_0}{h^2} \right) 4\alpha R^2 - \left(\frac{D \rho \rho_0 E}{h^2} \right) \frac{\partial R}{\partial Y} - \left(\frac{\rho \rho_0 \mu_0 \delta}{h} \right) \frac{\partial R}{\partial X}$$

which may be simplified

$$\left(\frac{\mu_0 h}{D} \right) \frac{U \partial R}{\partial X} = - 4\alpha R^2 - E \frac{\partial R}{\partial Y} - \left(\frac{\mu_0 h}{D} \right) \delta \frac{\partial R}{\partial X}$$

Substitute $\beta = \frac{\mu_0 h}{D}$

$$\beta U \frac{\partial R}{\partial X} = - 4\alpha R^2 - E \frac{\partial R}{\partial Y} - \beta \delta \frac{\partial R}{\partial X}$$

$$\beta (U + \delta) \frac{\partial R}{\partial X} = - E \frac{\partial R}{\partial Y} - 4\alpha R^2$$

Rearranging

$$(S + U) \frac{\partial R}{\partial \left(\frac{4\alpha X}{\beta} \right)} = - \left(\frac{E}{4\alpha} \right) \frac{\partial R}{\partial Y} - R^2$$

$$(S + U) \frac{\partial R}{\partial X_1^*} = - E^* \frac{\partial R}{\partial Y} - R^2$$

Where $X_1^* = \frac{4\alpha X}{\beta}$ and $E^* = \frac{E}{4\alpha}$ as for the case of electrostatic charge only.

Eq. 3-15 in non-dimensionalized form is the same as the previous case.

$$\frac{\partial E^*}{\partial Y} = R$$

4. Case of vertical tube flow considering diffusion and gravity.

$$u \frac{\partial p_p}{\partial x} + v \frac{\partial p_p}{\partial r} = \frac{D}{\lambda} \frac{\partial}{\partial \lambda} \left(\lambda \frac{\partial p_p}{\partial \lambda} \right) - \frac{\partial}{\partial x} (v_g p_p) \quad (4-5)$$

Using the dimensionless quantities in Appendix A we have

$$u \frac{\partial p_p}{\partial x} = u_0 \lambda \frac{p_{p0} \partial R}{\beta \lambda_0 \partial x}$$

$$v \frac{\partial p_p}{\partial r} = u_0 v \frac{p_{p0} \partial R}{\lambda_0 \partial \lambda^*}$$

$$\frac{D}{\lambda} \frac{\partial}{\partial \lambda} \left(\lambda \frac{\partial p_p}{\partial \lambda} \right) = \frac{D}{\lambda_0 \lambda^*} \frac{\partial}{\partial \lambda^*} \left(\lambda_0 \lambda^* \frac{p_{p0} \partial R}{\lambda_0 \partial \lambda^*} \right)$$

$$= \frac{D p_{p0}}{\lambda_0^2 \lambda^*} \frac{\partial}{\partial \lambda^*} \left(\lambda^* \frac{\partial R}{\partial \lambda^*} \right)$$

$$-\frac{\partial}{\partial x} (p_p v_g) = -\frac{p_{p0} v_g \partial R}{\beta \lambda_0 \partial x} = -\frac{p_{p0} u_0 v_g \partial R}{\beta \lambda_0 u_0 \partial x}$$

$$= -\frac{p_{p0} u_0 \delta \partial R}{\beta \lambda_0 \partial x}$$

Substituting into Eq. 4-5

$$\frac{u_0 \lambda p_{p0} \partial R}{\beta \lambda_0 \partial x} + \frac{u_0 v p_{p0} \partial R}{\lambda_0 \partial \lambda^*} = \frac{D p_{p0}}{\lambda_0^2 \lambda^*} \frac{\partial}{\partial \lambda^*} \left(\lambda^* \frac{\partial R}{\partial \lambda^*} \right) - \frac{p_{p0} u_0 \delta \partial R}{\beta \lambda_0 \partial x}$$

Multiply through by $\left(\frac{\lambda_0^2}{D p_{p0}} \right)$ and substitute $\beta = \left(\frac{u_0 \lambda_0}{D} \right)$

$$U \frac{\partial R}{\partial x} + \beta V \frac{\partial R}{\partial \pi^*} = \frac{1}{\lambda^*} \frac{\partial}{\partial \pi^*} \left(\lambda^* \frac{\partial R}{\partial \pi^*} \right) - \delta \frac{\partial R}{\partial x}$$

$$\lambda^* (\delta + U) \frac{\partial R}{\partial x} + \lambda^* \beta V \frac{\partial R}{\partial \pi^*} = \frac{\partial}{\partial \pi^*} \left(\lambda^* \frac{\partial R}{\partial \pi^*} \right) \quad (4-6)$$

The continuity equation is

$$\frac{\partial (u + v_g)}{\partial x} + \frac{1}{\lambda} \frac{\partial (\lambda v)}{\partial \pi} = 0 \quad (4-1)$$

Non-dimensionalize as follows.

$$\frac{\partial (u + v_g)}{\partial x} = \frac{\partial (u_0 U + u_0 \delta)}{\beta \lambda_0 \partial x} = \frac{u_0 \partial (\delta + U)}{\beta \lambda_0 \partial x}$$

$$\frac{1}{\lambda} \frac{\partial (\lambda v)}{\partial \pi} = \frac{1}{\lambda_0 \lambda^*} \frac{\partial \lambda_0 \lambda^* u_0 v}{\partial \lambda_0 \lambda^*} = \frac{u_0}{\lambda_0 \lambda^*} \frac{\partial \lambda^* v}{\partial \lambda^*}$$

Substituting

$$\frac{u_0}{\beta \lambda_0} \frac{\partial (\delta + U)}{\partial x} = \frac{u_0}{\lambda_0 \lambda^*} \frac{\partial \lambda^* v}{\partial \lambda^*}$$

$$\frac{1}{\beta} \frac{\partial (\delta + U)}{\partial x} + \frac{1}{\lambda^*} \frac{\partial \lambda^* v}{\partial \lambda^*} = 0 \quad (4-1a)$$

Equation 4-6 in conjunction with the continuity Eq. 4-1a may be written as

$$\frac{\partial}{\partial x} \left[(\delta + u) R \lambda^* \right] + \frac{\partial}{\partial \lambda^*} (\beta v R \lambda^*) = \frac{\partial}{\partial \lambda^*} \left(\lambda^* \frac{\partial R}{\partial \lambda^*} \right) \quad (4-7)$$

Since, expanding 4-7 we get

$$\begin{aligned} \lambda^* (\delta + u) \frac{\partial R}{\partial x} + R \frac{\partial}{\partial x} \left[(\delta + u) \lambda^* \right] + \lambda^* \beta v \frac{\partial R}{\partial \lambda^*} + R \frac{\partial (\lambda^* \beta v)}{\partial \lambda^*} \\ = \frac{\partial}{\partial \lambda^*} \left(\lambda^* \frac{\partial R}{\partial \lambda^*} \right) \end{aligned}$$

Divide through by λ^* and rearrange

$$\begin{aligned} \left(\delta + u \right) \frac{\partial R}{\partial x} + \beta v \frac{\partial R}{\partial \lambda^*} + \left\{ \frac{R}{\lambda^*} \frac{\partial}{\partial x} \left[(\delta + u) \lambda^* \right] + \frac{R}{\lambda^*} \frac{\partial (\lambda^* \beta v)}{\partial \lambda^*} \right\} \\ = \frac{1}{\lambda^*} \frac{\partial}{\partial \lambda^*} \left(\lambda^* \frac{\partial R}{\partial \lambda^*} \right) \end{aligned}$$

And from the continuity equation

$$\begin{aligned} \left\{ \frac{R}{\lambda^*} \frac{\partial}{\partial x} \left[(\delta + u) \lambda^* \right] + \frac{R}{\lambda^*} \frac{\partial (\lambda^* \beta u)}{\partial \lambda^*} \right\} \\ = \beta \frac{R}{\lambda^*} \left\{ \frac{\lambda^*}{\beta} \frac{\partial (\delta + u)}{\partial x} + \frac{(\delta + u) \partial \lambda^*}{\beta \partial x} + \frac{\partial (\lambda^* v)}{\partial \lambda^*} \right\} \\ = \beta \frac{R}{\lambda^*} \left\{ \frac{\lambda^*}{\beta} \frac{\partial (\delta + u)}{\partial x} + \frac{\partial (\lambda^* v)}{\partial \lambda^*} \right\} \end{aligned}$$

COMPUTER PROGRAM FOR CASE #1 - CHANNEL FLOW CONSIDERING
DIFFUSION AND ELECTROSTATIC CHARGE EFFECTS

$$\frac{U \partial R}{\partial X^*} = \frac{\partial^2 R}{\partial Y^2} - \frac{E \partial R}{\partial Y} - 4\alpha R^2 \quad (3-12)$$

$$\frac{\partial E}{\partial Y} = 4\alpha R \quad (3-13a)$$

These governing equations written in finite difference form are

$$U_{i,j} \left[\frac{R_{i+1,j} - R_{i,j}}{\Delta X^*} \right] = \frac{R_{i+1,j+1} - 2R_{i+1,j} + R_{i+1,j-1}}{\Delta Y^2} - E_{i,j} \left[\frac{R_{i+1,j+1} - R_{i+1,j-1}}{2\Delta Y} \right] - 4\alpha R_{i,j} (R_{i+1,j}) \quad (C-1)$$

$$\frac{E_{i+1,j+1} - E_{i+1,j}}{\Delta Y} = 4\alpha R_{i+1,j} \quad (C-2)$$

Expand these terms

$$\begin{aligned} & \frac{U_{i+1,j}}{\Delta X^*} [R_{i+1,j}] - \frac{U_{i+1,j}}{\Delta X^*} [R_{i,j}] - \frac{1}{\Delta Y^2} [R_{i+1,j+1}] + \frac{2}{\Delta Y^2} [R_{i+1,j}] \\ & - \frac{1}{\Delta Y^2} [R_{i+1,j-1}] + \frac{E_{i,j}}{2\Delta Y} [R_{i+1,j+1}] - \frac{E_{i,j}}{2\Delta Y} [R_{i+1,j-1}] \\ & + 4\alpha R_{i,j} [R_{i+1,j}] = 0 \end{aligned}$$

And

$$\frac{1}{\Delta Y} [E_{i+1,j+1}] - \frac{1}{\Delta Y} [E_{i+1,j}] = 4\alpha R_{i+1,j}$$

Simplify by letting $H = \Delta X$ and $S = \Delta Y$ and combine terms.

$$\begin{aligned} & - \left[\frac{1}{S^2\beta} + \frac{E_{i,j}}{2S\beta} \right] R_{i+1,j-1} \\ & + \left[\frac{U(N)}{H} + \frac{2}{S^2\beta} + \frac{4\alpha R_{i,j}}{\beta} \right] R_{i+1,j} + \left[\frac{E_{i,j}}{2S\beta} - \frac{1}{S^2\beta} \right] R_{i+1,j+1} \\ & = \left[\frac{U(N)}{H} \right] R_{i,j} \end{aligned} \tag{C-3}$$

$$\frac{1}{S} [E_{i+1,j+1}] - \frac{1}{S} [E_{i+1,j}] = [4\alpha] R_{i+1,j} \tag{C-4}$$

Let :

$$RA(N) = - \left[\frac{1}{s^2 \beta} + \frac{E_{i,j}}{2 s \beta} \right]$$

$$RB(N) = \left[\frac{U(N)}{H} + \frac{2}{s^2 \beta} + \frac{4\alpha}{\beta} E_{i,j} \right]$$

$$RC(N) = \left[\frac{E_{i,j}}{2 s \beta} - \frac{1}{s^2 \beta} \right]$$

$$RV(N) = \frac{1}{s}$$

$$RW(N) = - \frac{1}{s}$$

Rewriting Eq. (C-3) and (C-4)

$$\begin{aligned} RA(N) [R_{i+1, i-1}] + RB(N) [R_{i+1, j}] + RC(N) [R_{i+1, j+1}] \\ = \frac{U(N)}{H} [R_{i, j}] \end{aligned} \quad (C-5)$$

$$RV(N) [E_{i+1, j+1}] + RW(N) [E_{i+1, j}] = 4 * ALFA * R_{i+1, j} \quad (C-6)$$

Where $2 \ll j \ll 22$ and $2 \ll N \ll 22$

The finite difference coordinates were selected to correspond to the spatial coordinates such that $i = 1$ corresponds to $X = 0$ and $j = 1$ corresponds to $Y = 0$. The vertical increment for each step S was chosen as constant such that $S = 0.05$. The increments in X direction varied from $H = .001$ to $H = 1.0$

The computer flow chart is shown in Fig. 3.2

The quantities U , V , R , E , $ALFA$, and $Beta$ at each point j in column i are known. These are boundary conditions as given in Chapter 3. By the use of the finite difference equations as expressed in Eq. C-5 and C-6 the matrix equation

$$A_i X_{i+1} = B_i$$

is generated for all points j at axial position i .

A_i is the matrix of coefficients at position i

B_i is the column vector at axial position i

X_{i+1} is the variable column vector at axial position $i + 1$.

A_i and B_i are expressed in terms of the quantities U_i , V_i , E_i and R_i .

X_{i+1} is expressed in terms of U_{i+1} , V_{i+1} , E_{i+1} and R_{i+1} .

This matrix is sparse and appears in the tridiagonal form.

A computer program has been written to solve this program which uses Gaussian Elimination.

The subroutines formulated for the elimination procedure were LINAEQ which in turn calls upon other subroutines: LUDECO, which decomposes the matrix into a triangular matrix; ELIMIN, which performs the elimination part of $AX = B$; and REFINE, which refines the solution.

The fractional penetration at any axial distance from the entrance is expressed as

$$\int_0^1 URdY$$

This may be integrated using Simpson's Rule

$$\int = \frac{S}{3} \left(f_0 + f_n + 4 \sum_{\substack{j=1 \\ j \text{ ODD}}}^{n-1} f_j + 2 \sum_{\substack{j=2 \\ j \text{ EVEN}}}^{n-2} f_j \right)$$

The fractional deposition may then be found since fractional deposition = (1 - fractional penetration).

2. Case of channel flow considering electrostatic charge effect only.

The governing equations 3-16 and 3-17 can be written in finite difference form as follows:

$$U_{i+1,j} \left[\frac{R_{i+1,j} - R_{i,j}}{\Delta X_i^*} \right] = - E_{i,j}^* \left[\frac{R_{i+1,j} - R_{i+1,j-1}}{\Delta Y} \right] - [R_{i+1,j}]^2 \quad (C-7)$$

$$\frac{E_{i+1,j+1}^* - E_{i+1,j}^*}{\Delta Y} = R_{i+1,j} \quad (C-8)$$

Let : $S = \Delta Y$

Then, rearranging the terms in Eq. (C-7)

$$\begin{aligned} [S] R_{i+1,j}^2 + \left[U_{i+1,j} \cdot \frac{S}{\Delta X_i^*} + E_{i,j}^* \right] R_{i+1,j} \\ - \left[U_{i+1,j} \cdot \frac{S}{\Delta X_i^*} \right] R_{i,j} - [E_{i,j}^*] R_{i+1,j-1} = 0 \end{aligned} \quad (C-9)$$

Where : $2 \leq j \leq 82$

The finite difference coordinates were selected corresponding to the spacial coordinates such that $i = 1$ corresponds to $X = 0$ and $j = 2$ corresponds to $Y = 0$. For $0 \leq X_1^* \leq 0.04$, 81 mesh points were used across the flow from the centerline to the wall and S was held constant at 0.0125. ΔX_1^* varied from 0.0001 to 0.01.

For $X_1^* = 0.04$, 41 mesh points ($S = 0.025$) were used.

Eq. (C-9) may be written as

$$\left(\frac{A}{2}\right) R_{i+1,j}^2 + (B) R_{i+1,j} - \left(\frac{C}{2}\right) = 0$$

Where :

$$A = 2 \left[S \right]$$

$$B = \left[U_{i+1,j} \cdot \frac{S}{\Delta X_1^*} + E_{i,j}^* \right] R_{i+1,j}$$

$$C = 2 \left[U_{i+1,j} \cdot \frac{S}{\Delta X_1^*} \right] R_{i,j} - \left[E_{i,j}^* \right] R_{i+1,j-1}$$

Solving for $R_{i+1,j}$

$$R_{i+1,j} = \frac{-B + (B^2 + AC)^{1/2}}{A} \quad (C-10)$$

Eq. (C-10) is thus the explicit solution for $R_{i+1,j}$.

Having calculated $R_{i+1,j}$, the electrostatic field intensity may be calculated from Eq. (C-8) such that

$$E_{i+1, j+1} = 2R_{i+1,j} S + E_{i+1,j} \quad (3-19)$$

For the initial centerline condition:

$$j = 2$$

$$R_{i,2} = 1.0$$

$$E_{i+1,2} = 1.0$$

$$U_{i+1,2} = U_c$$

The fractional penetration at any axial distance from the entrance is $\int_0^1 URdY$, which is integrated using Simpson's Rule.

Referring back to the governing Eq. (C-7)

$$U_{i+1,2} \left(\frac{R_{i+1,2} - 1.0}{X_1^*} \right) = -0. - \left(R_{i+1,2} \right) R_{i,2}$$

$$R_{i+1,2} + \left(\frac{U_c}{X_1^*} \right) R_{i+1,2} - \left(\frac{U_c}{X_1^*} \right) = 0$$

$$R_{i+1,2} = \frac{1}{1 + \frac{X_1^*}{U_c}} \quad (C-11)$$

For the condition of uniform flow, $U_c = 1.0$ and (C-11) may be expressed as

$$R_{i+1,2} = \frac{1}{1 + X_1^*} \quad (C-12)$$

For channel flow the initial condition for the fraction of penetration is $\frac{\int_0^1 URdy}{\int_0^1 U_0 R_0 dy} = \frac{1}{1 + X_1^*}$ which is equal to Eq. (C-12).

3. Case of channel flow considering charge effect with gravity.

The governing equation (3-20) can be written in finite difference form as follows:

$$\begin{aligned} (\delta + U_{i+1,j}) \left[\frac{R_{i+1,j} - R_{i,j}}{\Delta x_i^*} \right] = - E_{i,j}^* \left[\frac{R_{i+1,j} - R_{i+1,j-1}}{\Delta Y} \right] \\ - \left[R_{i+1,j} \right]^2 \end{aligned} \quad (C-13)$$

and

$$\left[\frac{E_{i+1,j+1}^* - E_{i+1,j}^*}{\Delta Y} \right] = R_{i+1,j} \quad (C-14)$$

Rearranging the terms in Eq. (C-13)

$$\begin{aligned} R_{i+1,j}^2 + \left[\frac{\delta}{\Delta x_i^*} + \frac{U_{i+1,j}}{\Delta x_i^*} + \frac{E_{i,j}^*}{\Delta Y} \right] R_{i+1,j} \\ - \left[\frac{\delta}{\Delta x_i^*} (R_{i,j}) + \frac{U_{i+1,j}}{\Delta x_i^*} (R_{i,j}) + \frac{E_{i,j}^*}{\Delta Y} (R_{i+1,j-1}) \right] = 0 \end{aligned} \quad (C-15)$$

Similar to the other cases for parabolic flow the velocity profile is $U = 1.5 (1-Y^2)$ and for Uniform Flow $U = 1$.

Equation (C-15) may be rewritten as

$$\left(\frac{A}{2} \right) R_{i+1,j}^2 + (B) R_{i+1,j} - \frac{C}{2} = 0$$

Where :

$$A = 2$$

$$B = \left[\frac{S}{\Delta X,^*} + \frac{U_{i+1,j}}{\Delta X,^*} + \frac{E_{i,j}^*}{\Delta Y} \right]$$

$$C = 2 \left[\frac{S}{\Delta X,^*} (R_{i,j}) + \frac{U_{i+1,j}}{\Delta X,^*} (R_{i,j}) + \frac{E_{i,j}^*}{\Delta Y} (R_{i+1,j-1}) \right]$$

Solving for $R_{i+1,j}$ the solution was determined explicitly.

$$R_{i+1,j} = \frac{-B + (B + AC)^{1/2}}{A} \quad (C-16)$$

The fractional penetration at the corresponding axial distance from the entrance is expressed as $\int_0^1 U(N) \cdot R(N) \cdot dY$. This may be integrated by using Simpson's Rule, where N varies from 1 to 81.

Thus,

$$\int_0^1 f(N) \cdot dY \approx \frac{S}{15} \left\{ 14 \left[\frac{1}{2} (f_0 - f_n) + \sum_{\substack{j=2 \\ j \text{ EVEN}}}^{n-2} f_j \right] \right. \\ \left. + 16 \sum_{\substack{j=1 \\ j \text{ ODD}}}^{n-1} f_j + 5 (f'(a) - f'(b)) \right\}$$

Where :

$$f(N) = U(N) \cdot R(N) \quad 1 \leq N \leq 81$$

$$f(a) = U(1) \cdot R(1)$$

$$f(b) = U(81) \cdot R(81) = 0 \cdot R(81) \text{ (wall)}$$

$$f'(a) = 0 \quad \text{(symmetry at } \phi \text{)}$$

$$f'(b) = - \left[\frac{f(81) - f(80)}{S} \right]$$

$$S = \Delta Y$$

Using the same method as for the previous cases, eighty-one rectangular mesh points were selected at the entrance. The increments in the Y-direction were held constant with $\Delta Y = 0.0125$. The eighty-one mesh points were reduced to forty-one beyond the axial distance of X_1^* equal to 0.04 and $\Delta Y = 0.025$. In the axial direction the increments varied from $\Delta X_1^* = 0.0001$ to 0.01.

4. Case of vertical tube flow considering diffusion and gravity.

The governing equation is expressed as

$$\frac{\partial}{\partial X} \left[(\delta + U) R \lambda^* \right] + \frac{\partial}{\partial \lambda^*} (\beta V R \lambda^*) = \frac{\partial}{\partial \lambda^*} \left(\lambda^* \frac{\partial R}{\partial \lambda^*} \right) \quad (4-7)$$

Next, integrate with respect to r^* from $r^* = b_2$ to $r^* = b_3$ to give an approximate finite difference expression. Refer to Fig. 4.1 which shows a typical interior control volume with a radial increment of S_3 and an axial increment of H .

Integrating the First Term

$$\int_2^3 \frac{\partial}{\partial x} \left[\overline{(\delta + U) R} \lambda^* \right] d\lambda^* = \frac{1}{dx} \int_2^3 \left[\overline{(\delta + U) R} \lambda^* \right] d\lambda^*$$

Where $\overline{(\delta + U) R}$ = average value at center of control volume

$$= \frac{1}{H} \left[(\delta + U_{2,3}) R_{2,3} \lambda_3^* - (\delta + U_{1,3}) R_{1,3} \lambda_3^* \right] S_3$$

$$= \left[(\delta + U_{2,3}) R_{2,3} \lambda_3^* - (\delta + U_{1,3}) R_{1,3} \lambda_3^* \right] \frac{S_3}{H}$$

Integrating the Second Term

$$\int_2^3 \frac{\partial}{\partial \lambda^*} \left[\beta V R \lambda^* \right] d\lambda^* = \left[\beta V R \lambda^* \right] \Bigg|_{\text{average on 2}}^{\text{average on 3}}$$

$$= \left[\beta V_3 \overbrace{R_3}^{\text{average on 3}} b_3 - \beta V_2 \overbrace{R_2}^{\text{average on 2}} b_2 \right]$$

Integrating the Third Term

$$\int_2^3 \frac{\partial}{\partial r^*} \left[r^* \frac{\partial R}{\partial r^*} \right] dr^* = \left[r^* \frac{\partial R}{\partial r^*} \right] \Bigg|_{\text{average on 2}}^{\text{average on 3}}$$

$$= \left[b_3 \frac{\left[\frac{(R_{2,4} - R_{2,3}) + (R_{1,4} - R_{1,3})}{2} \right]}{\frac{S_3}{2} + \frac{S_4}{2}} \right]$$

$$- \left[b_2 \frac{\left[\frac{(R_{2,3} - R_{2,2}) + (R_{1,3} - R_{1,2})}{2} \right]}{\frac{S_2}{2} + \frac{S_3}{2}} \right]$$

$$= b_3 \frac{[R_{2,4} - R_{2,3} + R_{1,4} - R_{1,3}]}{S_3 + S_4} - b_2 \frac{[R_{2,3} - R_{2,2} + R_{1,3} - R_{1,2}]}{S_2 + S_3}$$

Combining the three terms

$$\begin{aligned} & \left[(\delta + U_{2,2}) R_{2,3} \lambda_3^* - (\delta + U_{1,3}) R_{1,3} \lambda_3^* \right] \frac{S_3}{H} \\ & + \left[\beta V_3 \bar{R}_3 b_3 - \beta V_2 \bar{R}_2 b_2 \right] \\ & = b_3 \frac{[R_{2,4} - R_{2,3} + R_{1,4} - R_{1,3}]}{S_3 + S_4} - b_2 \frac{[R_{2,3} - R_{2,2} + R_{1,3} - R_{1,2}]}{S_2 + S_3} \end{aligned}$$

Rearranging,

$$\begin{aligned} & \lambda_3^* S_3 (\delta + U_{2,3}) R_{2,3} - \lambda_3^* S_3 (\delta + U_{1,3}) R_{1,3} \\ & + \beta H b_3 V_3 \bar{R}_3 - \beta H b_2 V_2 \bar{R}_2 \\ & = \frac{H b_3}{S_3 + S_4} (R_{2,4} - R_{2,3} + R_{1,4} - R_{1,3}) \\ & - \frac{H b_2}{S_2 + S_3} (R_{2,3} - R_{2,2} + R_{1,3} - R_{1,2}) \end{aligned} \tag{C-17}$$

\bar{R}_3 and \bar{R}_2 are average values of R along the control surface b_3 and b_2 respectively. \bar{R}_3 may be found by linear interpolation as follows: (refer to Fig. 4.1)

$$\bar{R}_3 = \frac{R_{1,4} + R_{2,4}}{2} + \frac{\frac{S_4}{2}}{\frac{S_3}{2} + \frac{S_4}{2}} \left[\frac{R_{1,3} + R_{2,3}}{2} - \frac{R_{1,4} + R_{2,4}}{2} \right]$$

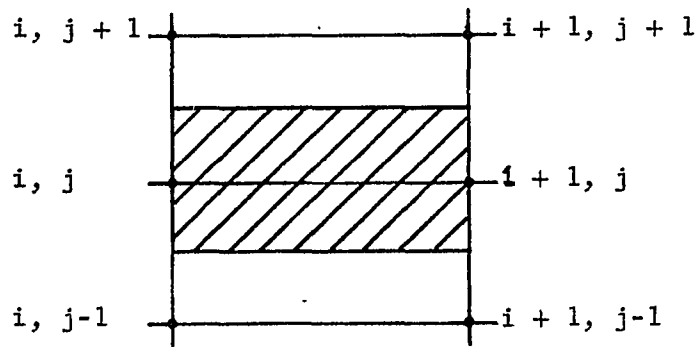
$$\bar{R}_3 = \frac{1}{2} \left[R_{2,4} + R_{1,4} + (R_{2,3} - R_{2,4} + R_{1,3} - R_{1,4}) \frac{S_4}{S_3 + S_4} \right] \quad (C-18)$$

Similarly,

$$\bar{R}_2 = \frac{R_{1,3} + R_{2,3}}{2} + \frac{\frac{S_3}{2}}{\frac{S_2}{2} + \frac{S_3}{2}} \left[\frac{R_{1,2} + R_{2,3}}{2} - \frac{R_{1,3} + R_{2,3}}{2} \right]$$

$$\bar{R}_2 = \frac{1}{2} \left[R_{2,3} + R_{1,3} + (R_{2,2} - R_{2,3} + R_{1,2} - R_{1,3}) \frac{S_3}{S_2 + S_3} \right] \quad (C-19)$$

Eq. (C-17) may be written using a finite difference grid as follows



$$\begin{aligned}
& \lambda_j^* S_j (S + U_{i+1,j}) R_{i+1,j} - \lambda_j^* S_j (S + U_{i,j}) R_{i,j} \\
& + \beta H b_j V_j \bar{R}_j - \beta H b_{j-1} V_{j-1} \bar{R}_{j-1} \\
& = \frac{H b_j}{S_j + S_{j+1}} (R_{i+1,j+1} - R_{i+1,j} + R_{i,j+1} - R_{i,j}) \\
& - \frac{H b_{j-1}}{S_{j-1} + S_j} (R_{i+1,j} - R_{i+1,j-1} + R_{i,j} - R_{i,j-1}) \tag{C-20}
\end{aligned}$$

Next, Eq. (C-18)

$$\begin{aligned}
\bar{R}(j) = & \left[\frac{R_{i+1,j+1}}{2} + \frac{R_{i,j+1}}{2} + (R_{i+1,j} - R_{i+1,j+1} + R_{i,j} \right. \\
& \left. - R_{i,j+1}) \frac{S_{j+1}}{2(S_j + S_{j+1})} \right] \tag{C-21}
\end{aligned}$$

Then, Eq. (C-19)

$$\begin{aligned}
\bar{R}(j-1) = & \left[\frac{R_{i+1,j}}{2} + \frac{R_{i,j}}{2} + (R_{i+1,j-1} - R_{i+1,j} + R_{i,j-1} \right. \\
& \left. - R_{i,j}) \frac{S_j}{2(S_{j-1} + S_j)} \right] \tag{C-22}
\end{aligned}$$

Finally, expanding the terms of Equation C-20, C-21, C-22 and rearranging:

$$\begin{aligned}
& - \left[\frac{H b_{j-1}}{S_{j-1} + S_j} + \frac{\beta H b_{j-1} V_{j-1} S_j}{2(S_{j-1} + S_j)} \right] R_{i+1, j-1} \\
& + \left[\lambda_j^* S_j (\delta + U_{i+1, j}) + \frac{\beta H b_j V_j S_{j+1}}{2(S_j + S_{j+1})} - \frac{\beta H b_{j-1} V_{j-1}}{2} \right. \\
& + \left. \frac{\beta H b_{j-1} V_{j-1} S_j}{2(S_{j-1} + S_j)} + \frac{H b_j}{(S_j + S_{j+1})} + \frac{H b_{j-1}}{(S_{j-1} + S_j)} \right] R_{i+1, j} \\
& + \left[\frac{\beta H b_j V_j}{2} - \frac{\beta H b_j V_j S_{j+1}}{2(S_j + S_{j+1})} - \frac{H b_j}{(S_j + S_{j+1})} \right] R_{i+1, j+1} \\
& = \left[\frac{H b_{j-1}}{(S_{j-1} + S_j)} + \frac{\beta H b_{j-1} V_{j-1} S_j}{2(S_{j-1} + S_j)} \right] R_{i, j-1} \\
& + \left[\lambda_j^* S_j (\delta + U_{i, j}) + \frac{\beta H b_{j-1} V_{j-1}}{2} - \frac{\beta H b_{j-1} V_{j-1} S_j}{2(S_{j-1} + S_j)} \right.
\end{aligned}$$

$$\begin{aligned}
& - \left[\frac{H b_j}{(S_j + S_{j+1})} - \frac{\beta H b_j V_j S_{j+1}}{2(S_j + S_{j+1})} - \frac{H b_{j-1}}{(S_{j-1} + S_j)} \right] R_{i,j} \\
& + \left[- \frac{\beta H b_j V_j}{2} + \frac{\beta H b_j V_j S_{j+1}}{2(S_j + S_{j+1})} - \frac{H b_j}{(S_j + S_{j+1})} \right] R_{i,j+1} \quad (4-9)
\end{aligned}$$

The fractional penetration of the particle phase at any given axial distance is

$$\frac{\int_0^{r_0} (v_g + u) \beta 2 \pi r dr}{(v_g + u_0) \pi r_0^2 \rho_0} \quad (C-23)$$

Non-dimensionalize as follows:

$$\delta = \frac{v_g}{u_0} \quad U = \frac{u}{u_0} \quad r^* = \frac{r}{r_0}$$

Substituting:

$$\begin{aligned}
& = \frac{\int (\delta + U) R 2 \pi r_0 r^* dr^*}{(\delta + 1) \pi r_0^2} \\
& = \frac{2 \int (\delta + U) R r^* dr^*}{(\delta + 1)}
\end{aligned}$$

The fractional deposition is then

$$1 - \frac{2 \int (\delta + L) R \lambda^* d\lambda^*}{(\delta + 1)}$$

(4-10)

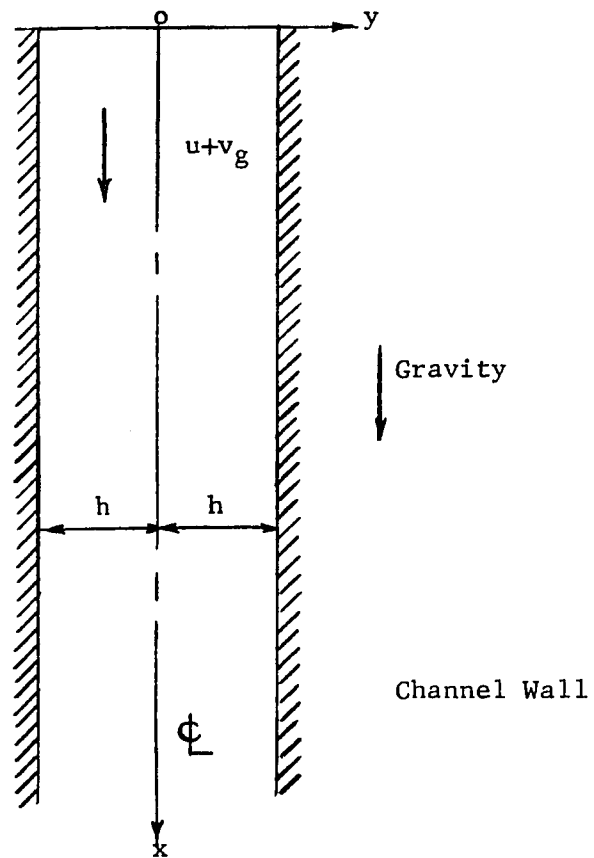


FIG. 3.1 VERTICAL PARALLEL PLATE CHANNEL CONFIGURATION

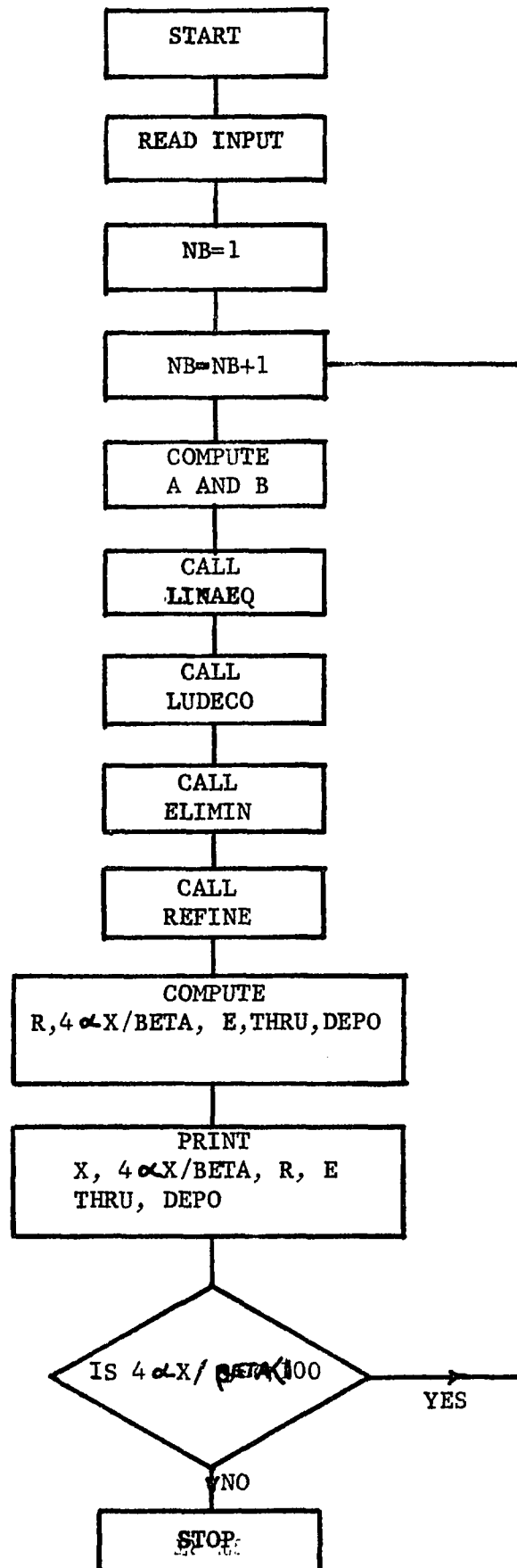


FIG. 3.2 COMPUTER FLOW CHART FOR FLOW IN A PARALLEL PLATE CHANNEL FOR DIFFUSION AND ELECTROSTATIC CHARGE.

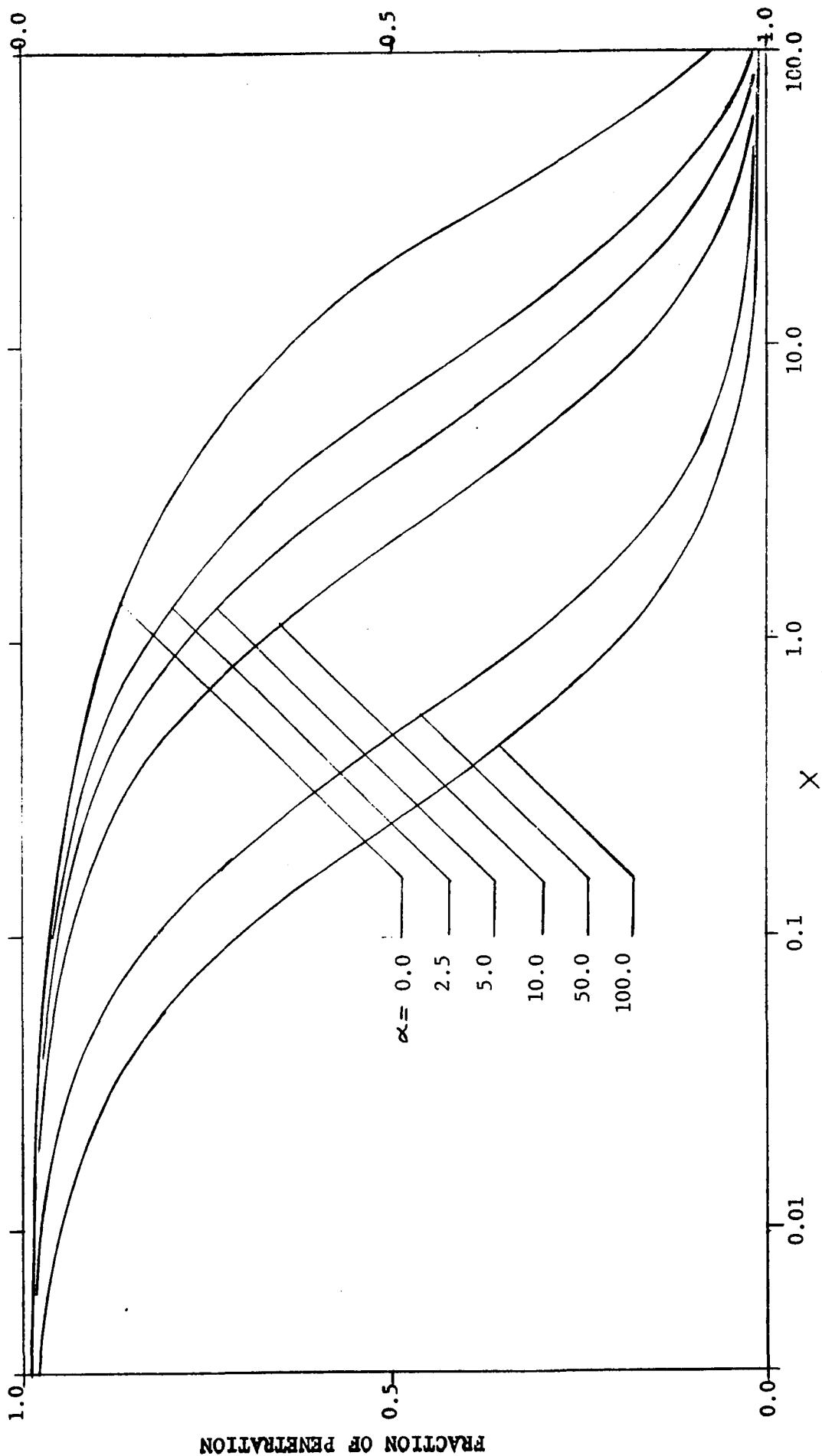


FIG. 3.3 AXIAL DISTRIBUTION OF FRACTION OF PENETRATION DUE TO DIFFUSION AND CHARGE EFFECT FOR UNIFORM FLOW IN A CHANNEL WITH X AS AXIAL PARAMETER.

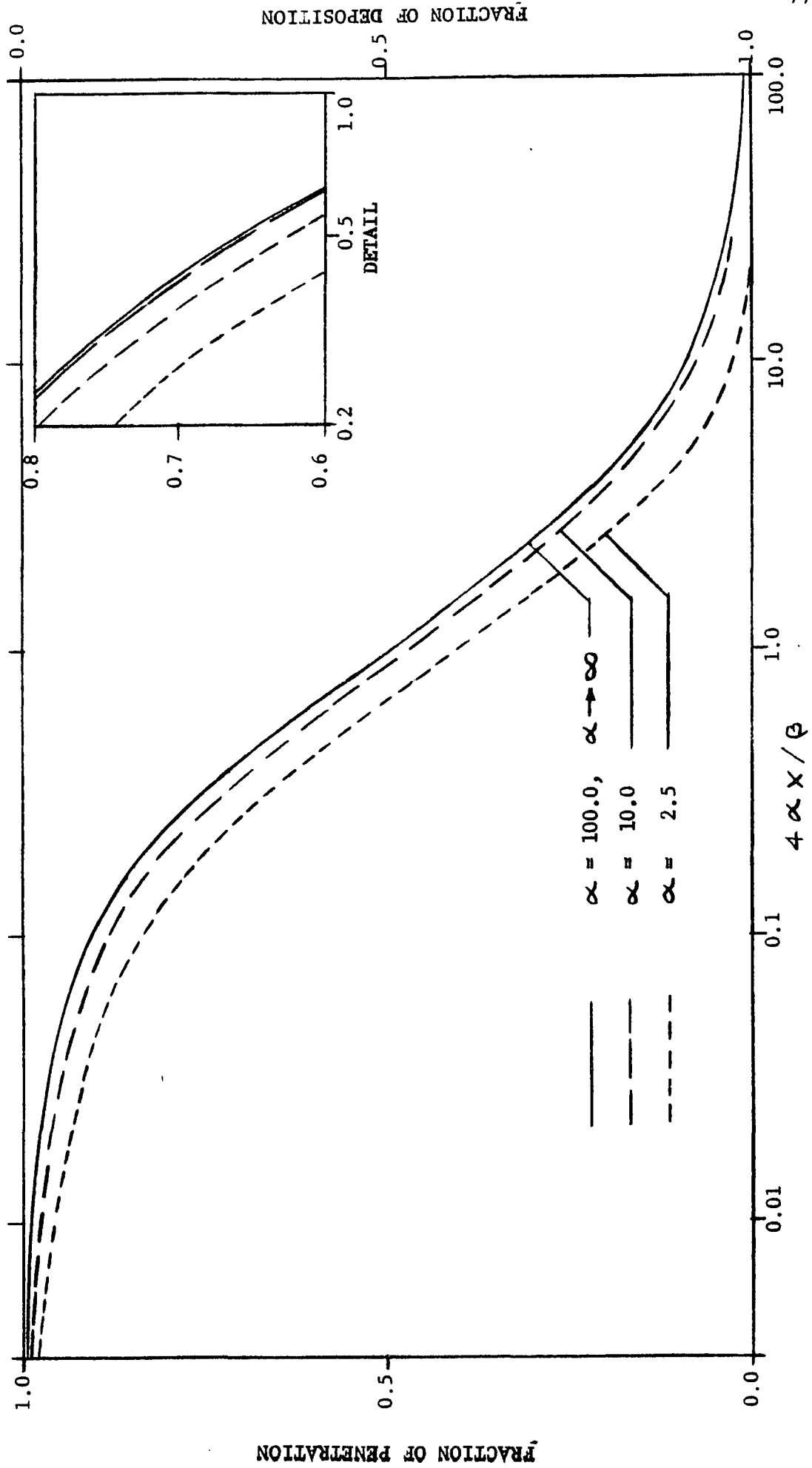


FIG. 3.4 AXIAL DISTRIBUTION OF FRACTION OF PENETRATION DUE TO DIFFUSION AND CHARGE EFFECT FOR UNIFORM FLOW IN A CHANNEL WITH $4 \alpha x / \beta$ AS AXIAL PARAMETER.

FRACTION OF PENETRATION

FRACTION OF DEPOSITION

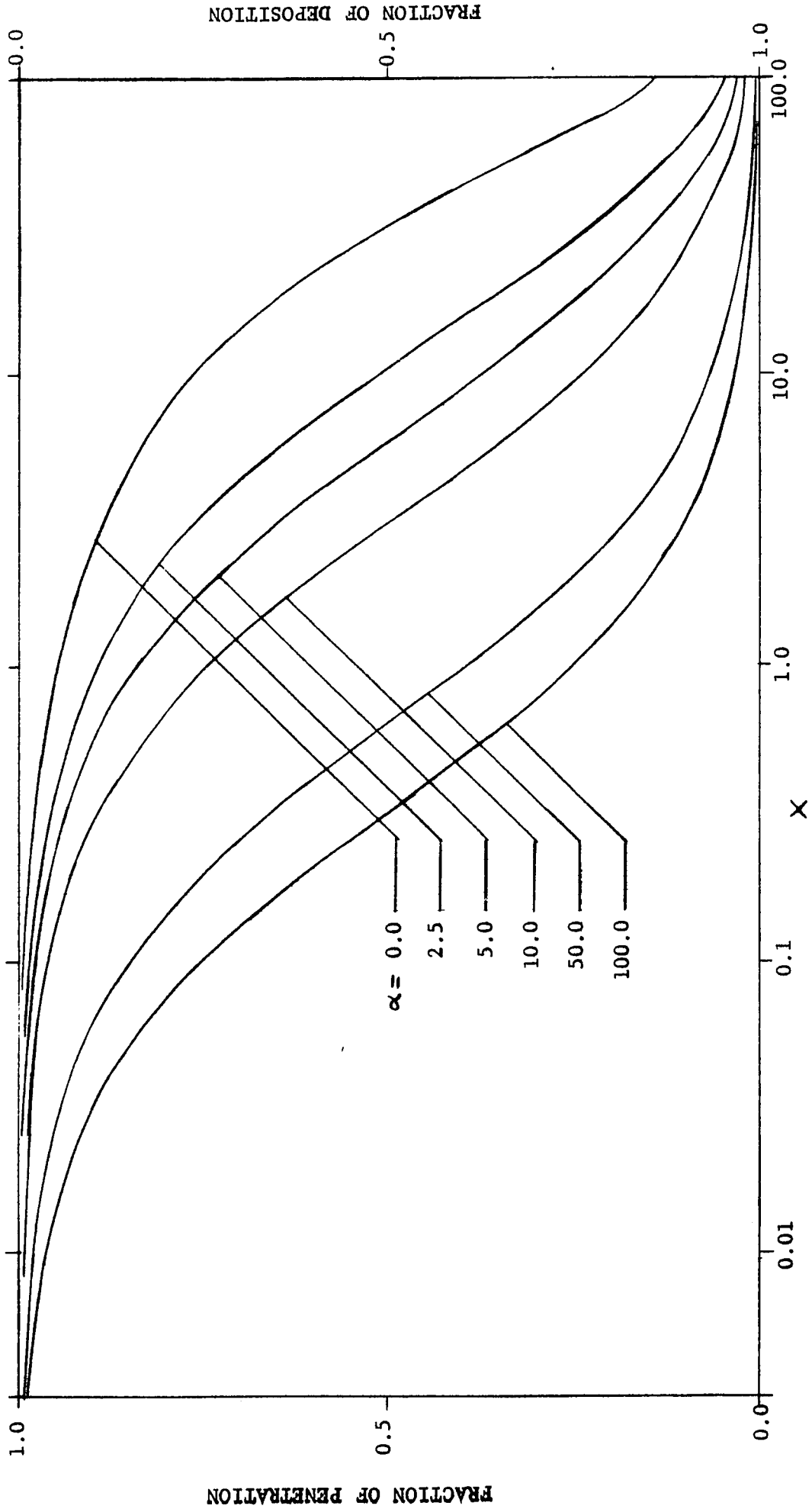
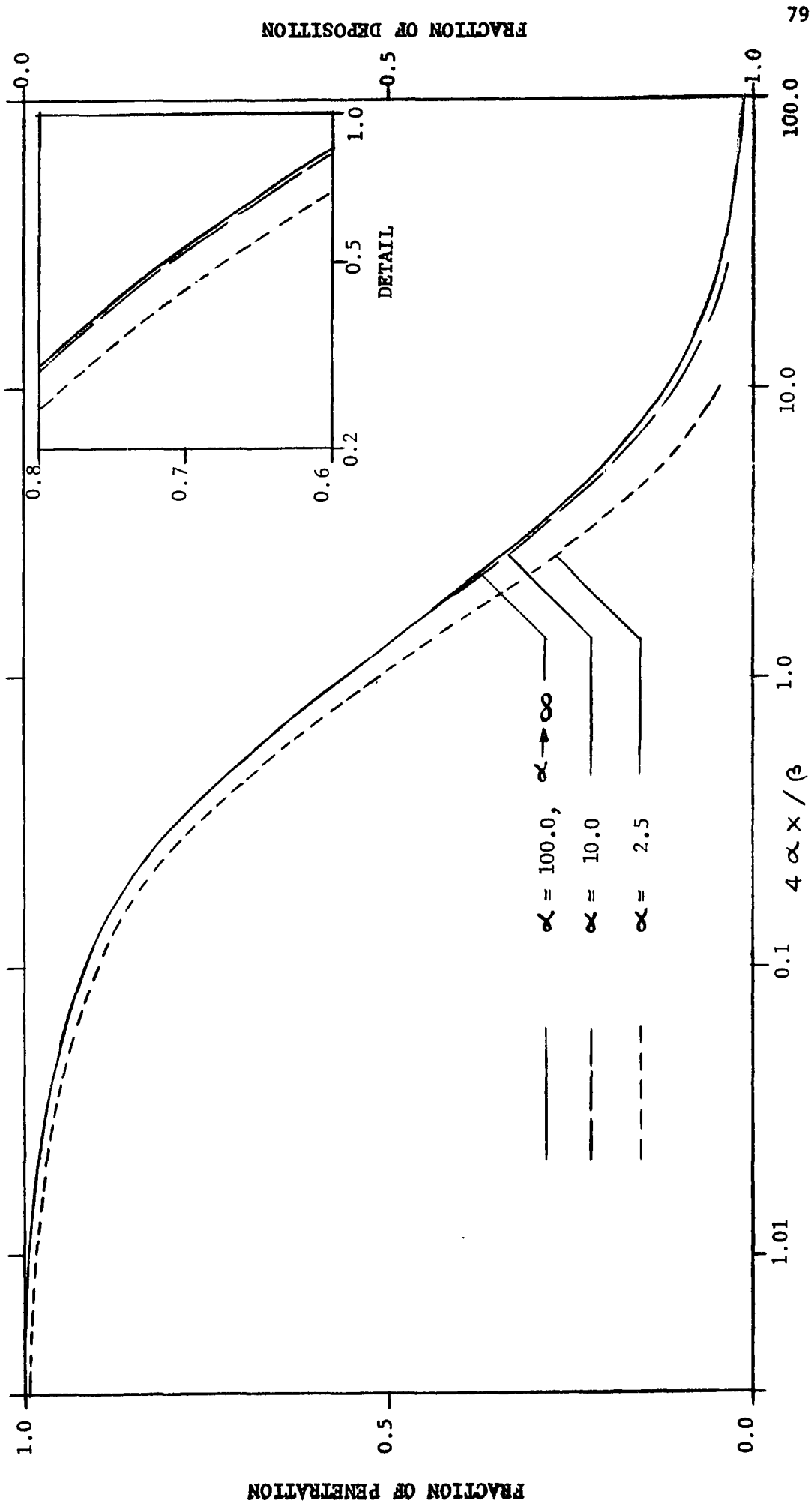


FIG. 3.5 AXIAL DISTRIBUTION OF FRACTION OF PENETRATION DUE TO DIFFUSION AND CHARGE EFFECT FOR PARABOLIC FLOW IN A CHANNEL WITH X AS AXIAL PARAMETER.

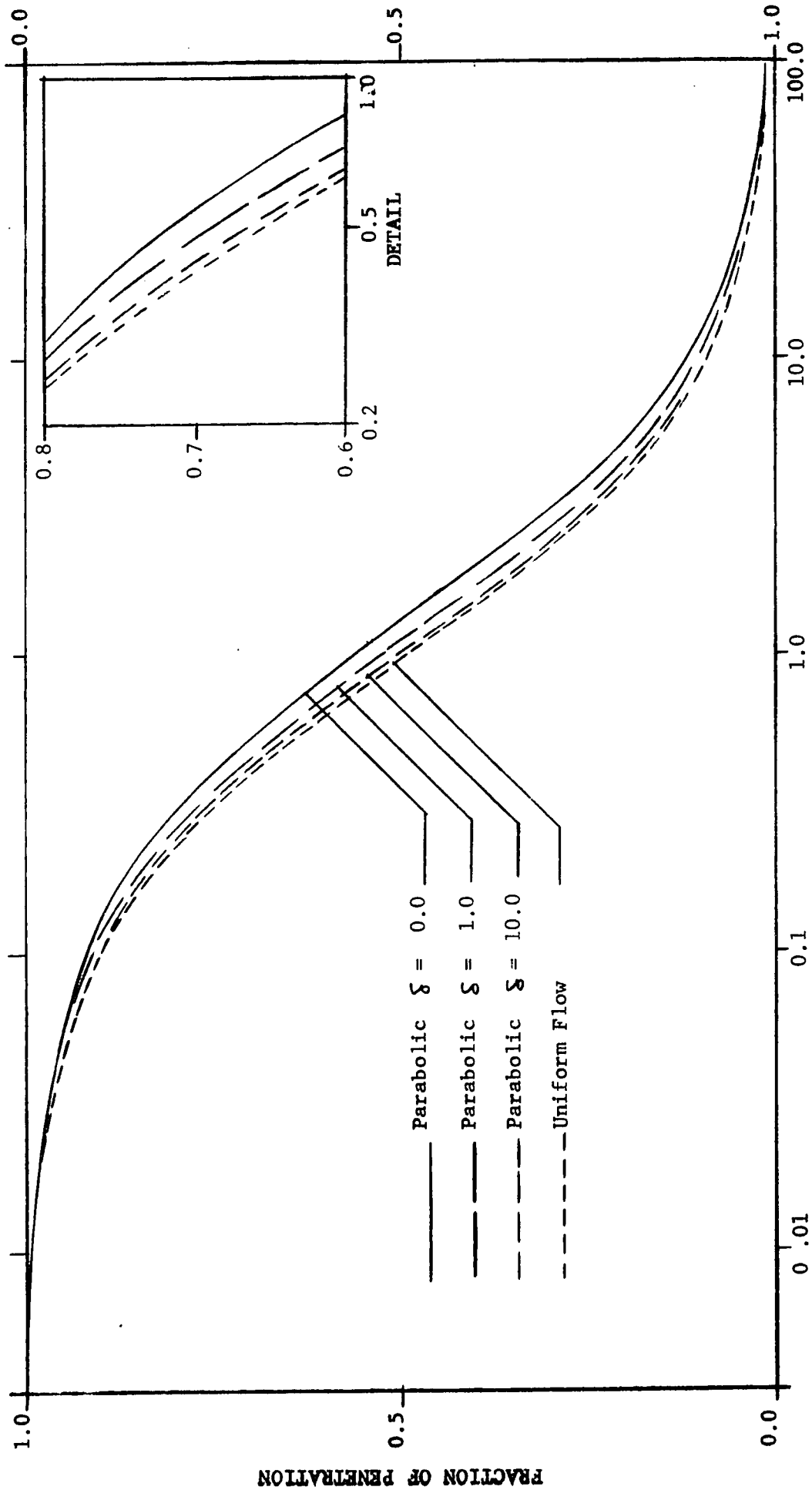
FRACTION OF DEPOSITION

FRACTION OF PENETRATION



79

FIG. 3.6 AXIAL DISTRIBUTION OF FRACTION OF PENETRATION DUE TO DIFFUSION AND CHARGE EFFECT FOR PARABOLIC FLOW IN A CHANNEL WITH $4\alpha x / \beta$ AS AXIAL PARAMETER.



FRACTION OF DEPOSITION

FIG. 3.7 AXIAL DISTRIBUTION OF FRACTION OF PENETRATION DUE TO CHARGE AND GRAVITY EFFECTS IN A VERTICAL CHANNEL.

FRACTION OF PENETRATION

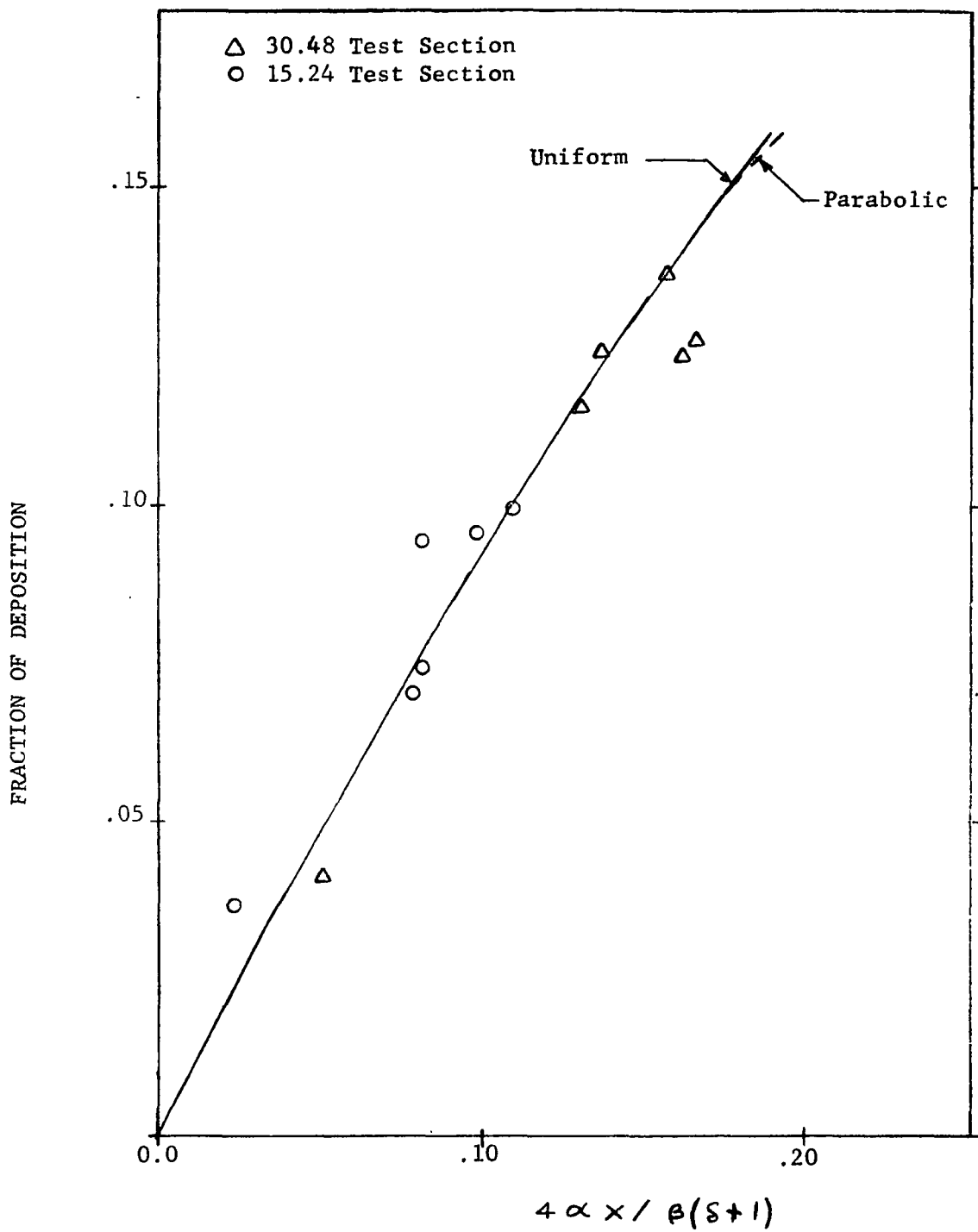


FIG. 3.8 COMPARISON OF EXPERIMENTAL DATA WITH THEORETICAL ANALYSIS FOR FRACTION OF DEPOSITION DUE TO CHARGE AND GRAVITY EFFECT FOR VERTICAL TUBE FOR UNIFORM FLOW AND PARABOLIC FLOW [28].

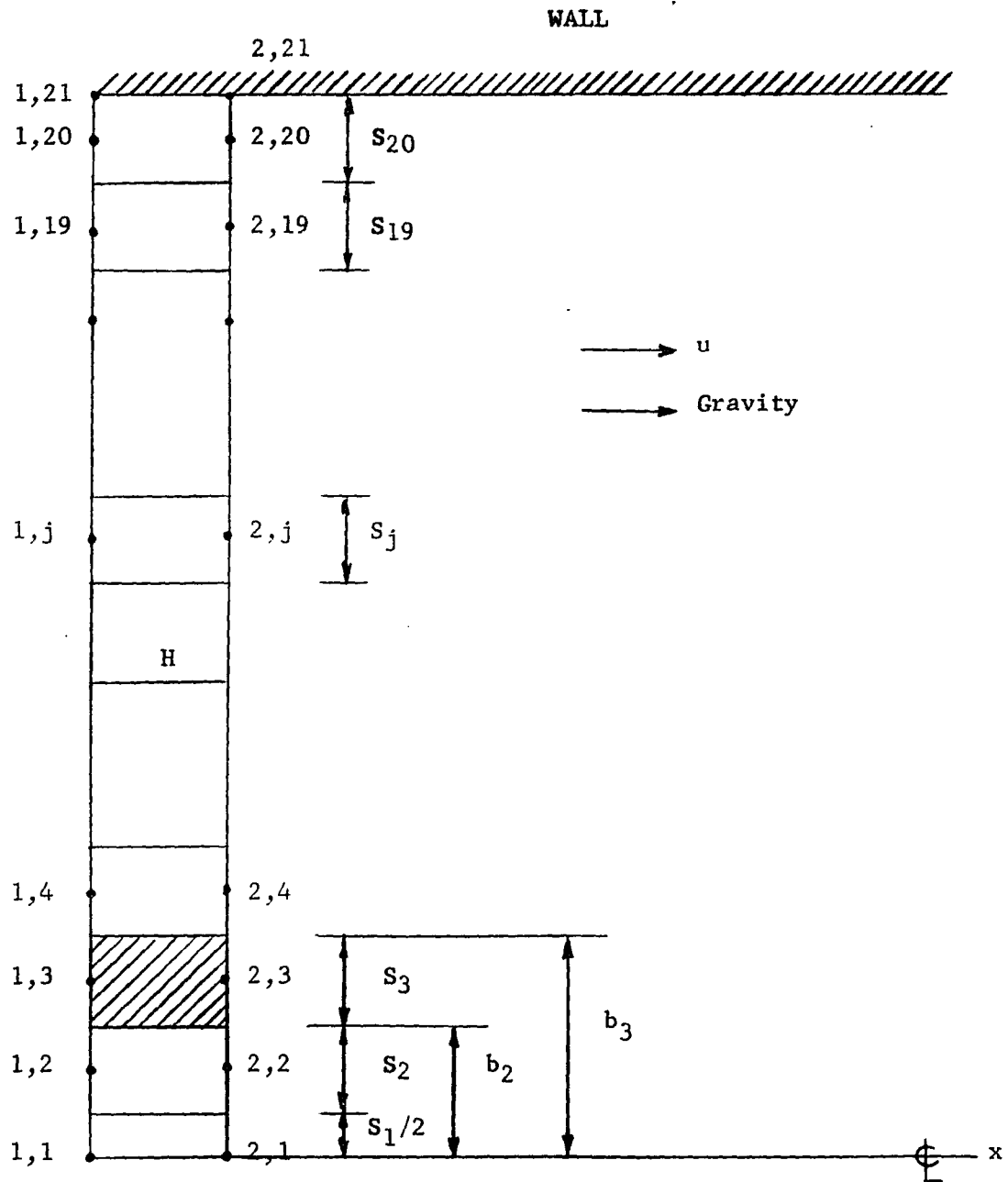


FIG. 4.1 FINITE DIFFERENCE REPRESENTATION OF FLOW FIELD
SHOWING AXIAL AND RADIAL INCREMENTS.

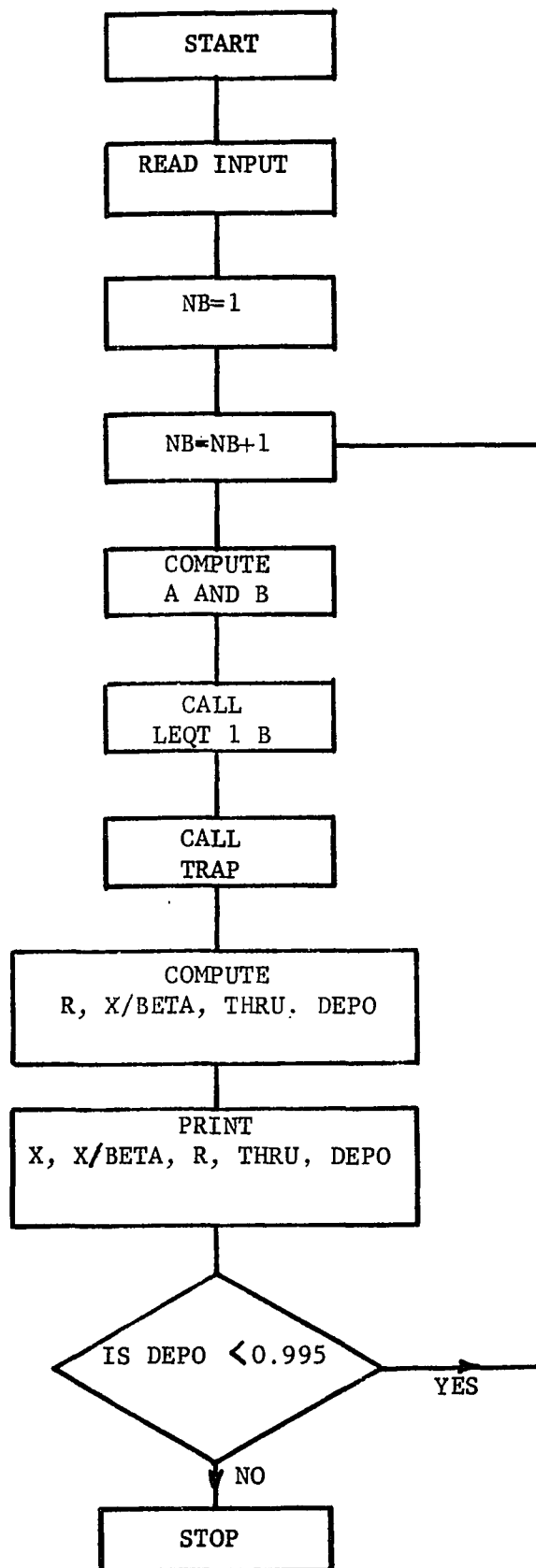


FIG. 4.2 COMPUTER FLOW CHART FOR FLOW IN A VERTICAL CIRCULAR TUBE WITH DIFFUSION AND GRAVITY EFFECTS.

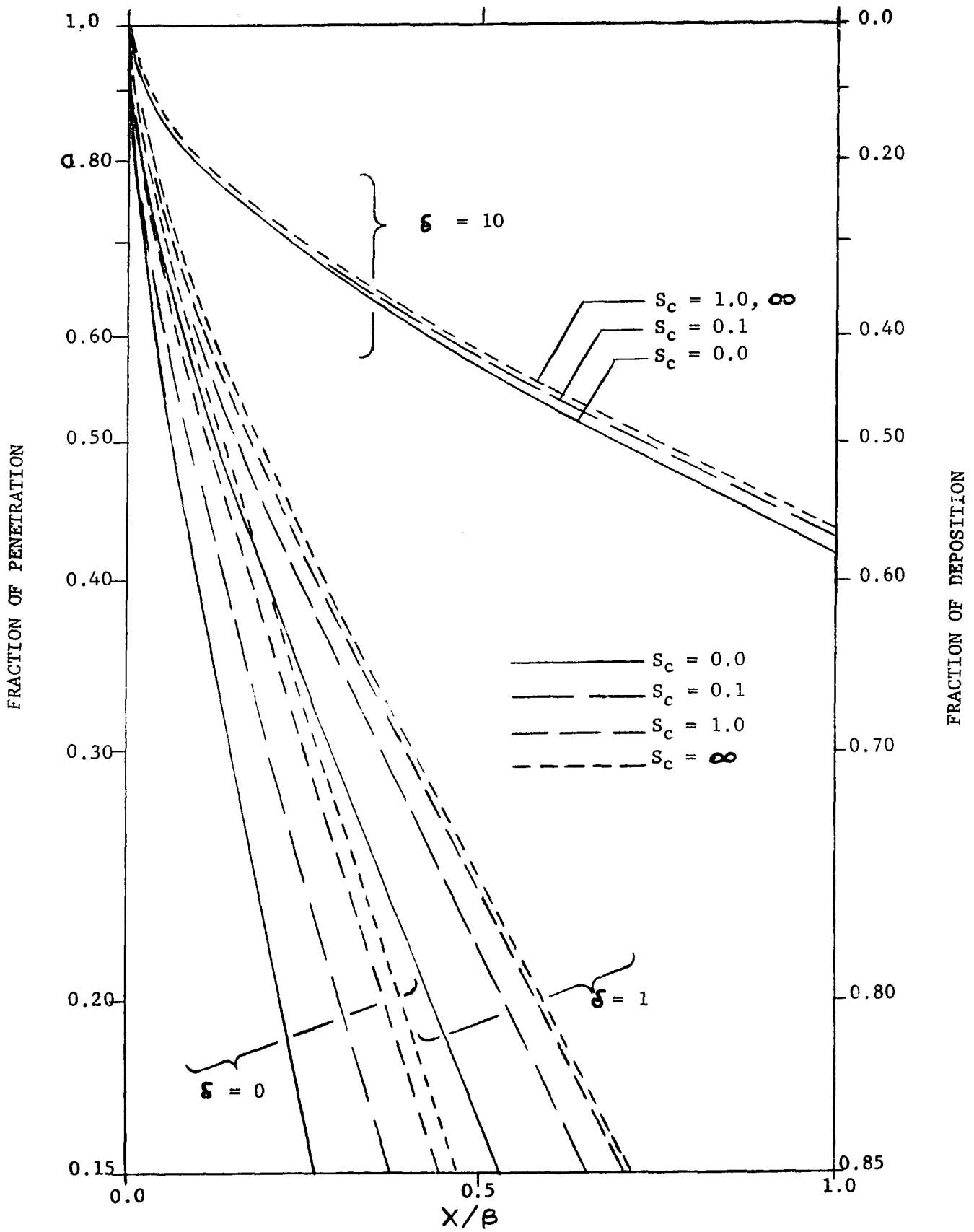


FIG. 4.3 AXIAL DISTRIBUTION OF FRACTION OF DEPOSITION WITH VARYING GRAVITY FLOW PARAMETERS OF $\delta = 0, 1, 10$ AND VARYING SCHMIDT NUMBERS OF $Sc = 0.0, 0.1, 1.0, \text{ AND } \infty$ FOR FLOW IN A CIRCULAR TUBE.

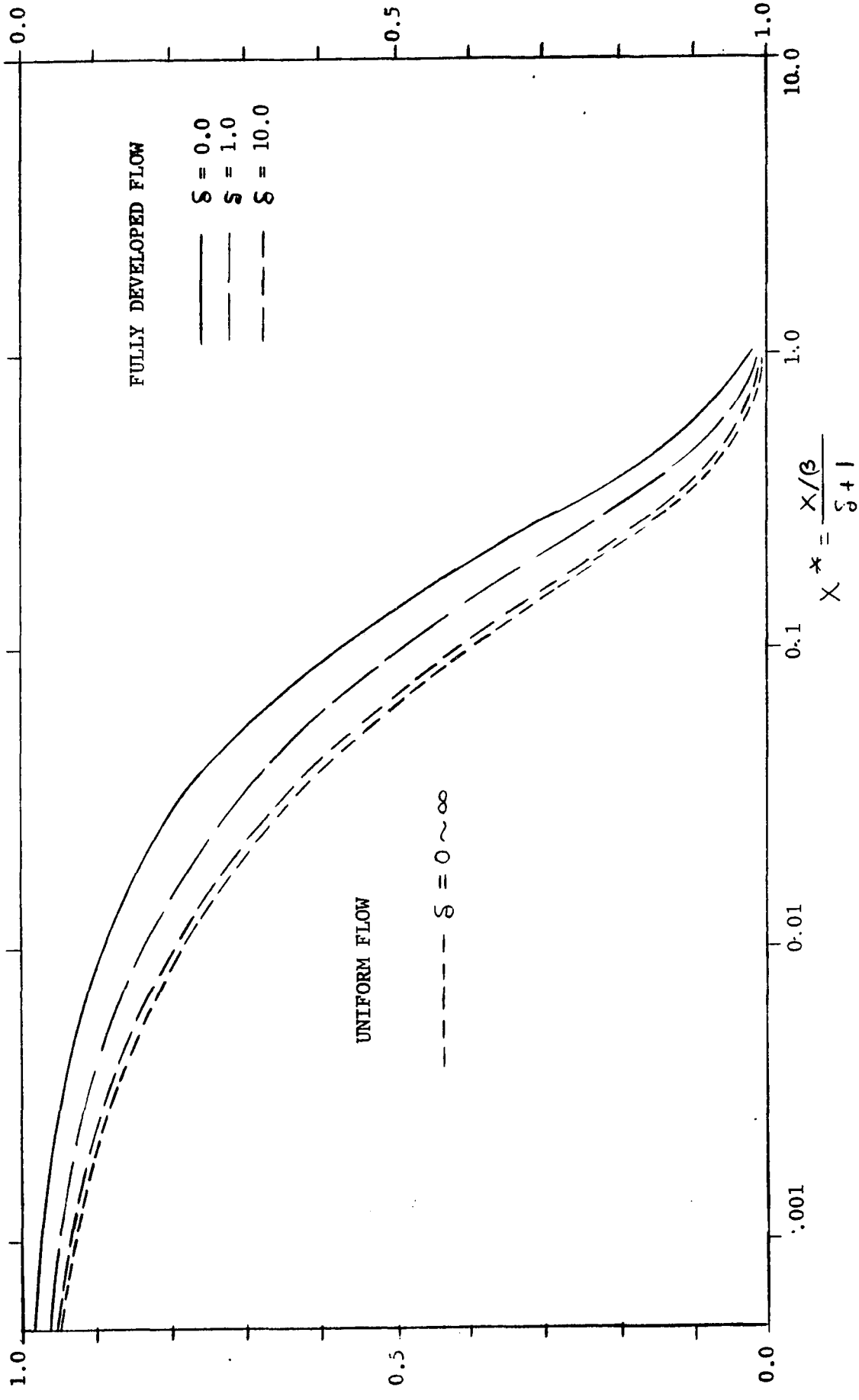


FIG. 4.4 AXIAL DISTRIBUTION OF FRACTION OF PENETRATION WITH VARYING VELOCITY RATIO PARAMETER FOR FULLY DEVELOPED FLOW AND WITH UNIFORM FLOW IN A CIRCULAR TUBE.

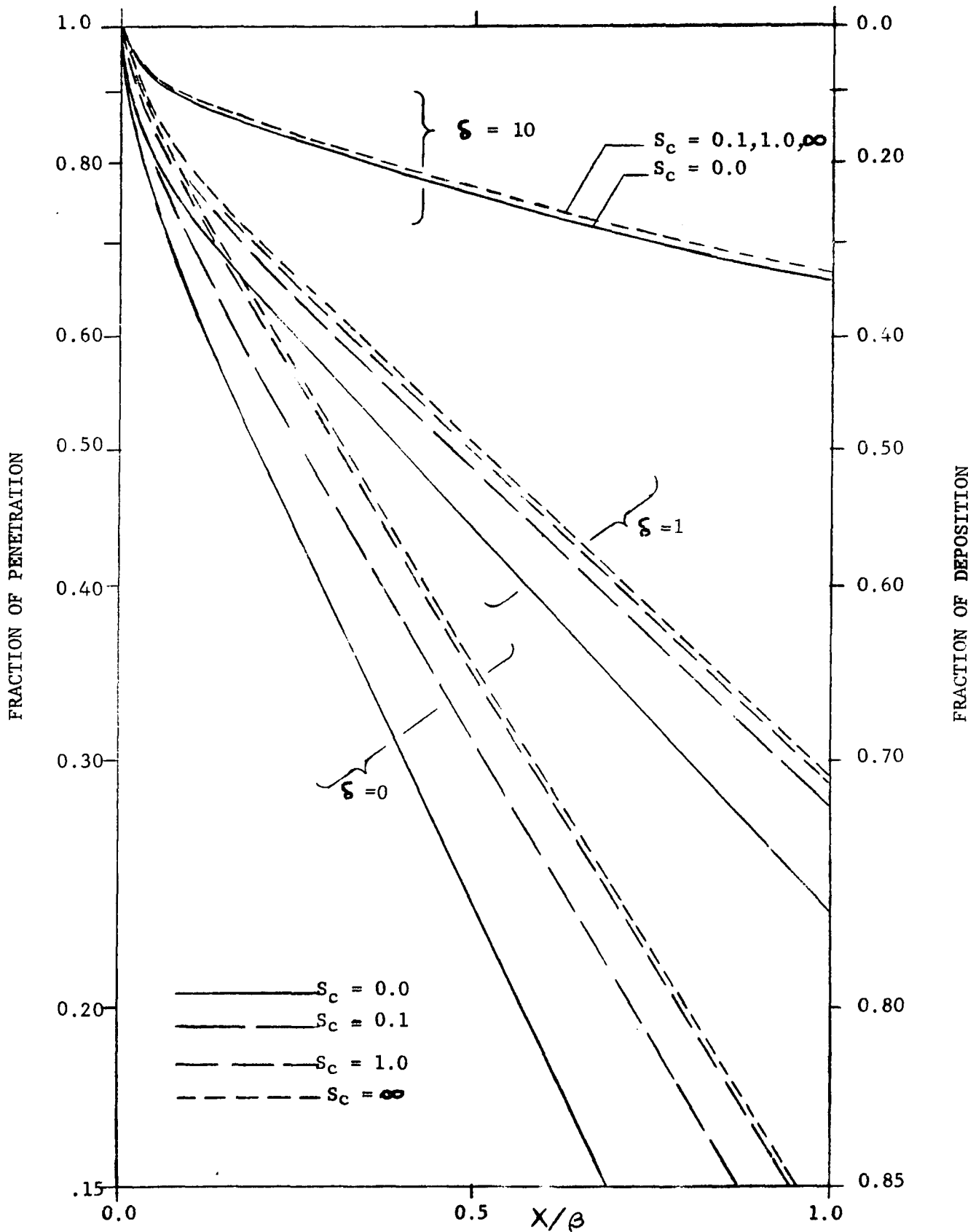


FIG. 4.5 AXIAL DISTRIBUTION OF FRACTION OF DEPOSITION WITH VARYING GRAVITY FLOW PARAMETERS OF $\delta = 0, 1, 10$ AND VARYING SCHMIDT NUMBERS OF $S_c = 0.0, 0.1, 1.0, \text{ AND } \infty$ FOR FLOW IN A PARALLEL PLATE CHANNEL.

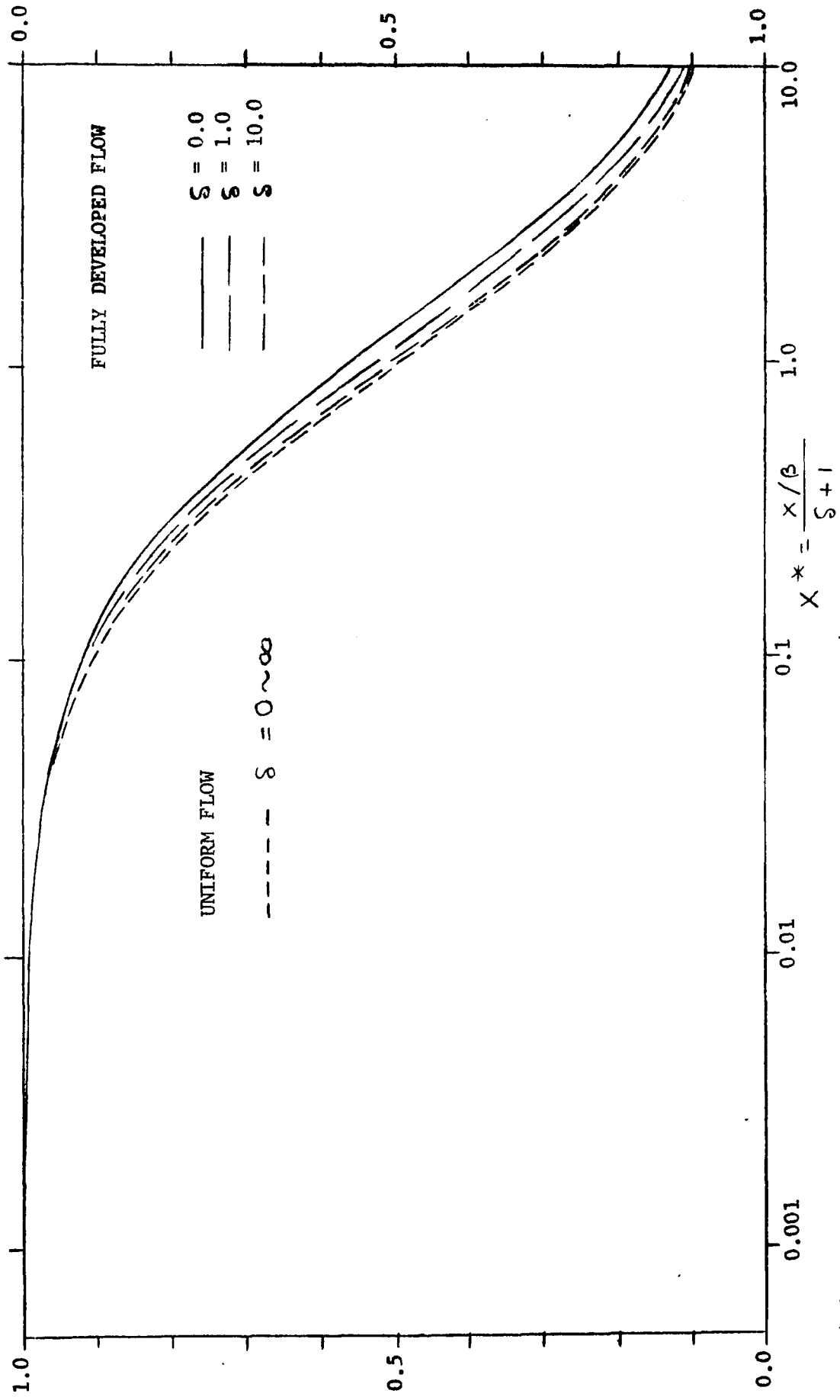


FIG. 4.6 AXIAL DISTRIBUTION OF FRACTION OF PENETRATION WITH VARYING VELOCITY RATIO PARAMETER FOR FULLY DEVELOPED FLOW AND WITH UNIFORM FLOW IN A PARALLEL PLATE CHANNEL.

FRACTION OF DEPOSITION

FRACTION OF PENETRATION

VITA

Melvin Wilbur Gelber was born in New Jersey. He received his B.S. in Mechanical Engineering, Magna Cum Laude, at the University of Notre Dame in 1944 and his M.S. in Mechanical Engineering at Notre Dame in 1947.

He served in the U.S.N.R. 1943-1946, with active duty in the Asiatic-Pacific Theater. He was an instructor in engineering mechanics at Notre Dame, 1947-1948; a stress analyst at Wright Aircraft Corp., Woodridge, New Jersey, 1948-1949 and an instructor in thermodynamics, heat and power at Cooper Union, New York, 1950-1951. He is a consulting engineer for the design of mechanical systems for the construction of buildings, 1950-present.

A member of Tau Beta Pi, Indiana Gamma. He is a member of the New Jersey Society of Professional Engineers, the National Society of Professional Engineers, licensed in New Jersey, New York, Connecticut, and has a National registration.